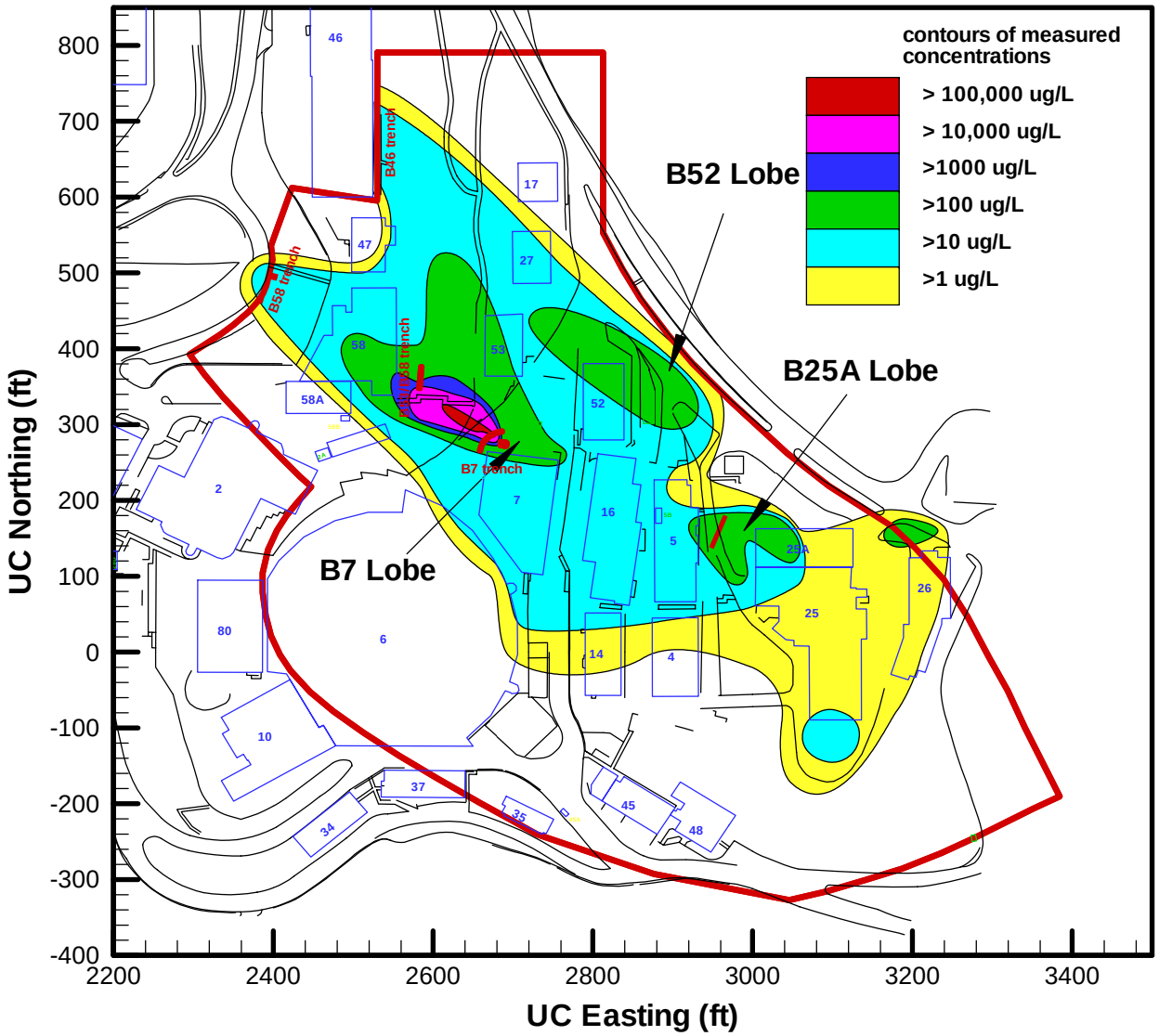

Figure 1. The Old Town map with buildings and their numbers in blue polygons and roads in black lines, and contaminant plumes measured in 1999 and groundwater collection trenches.

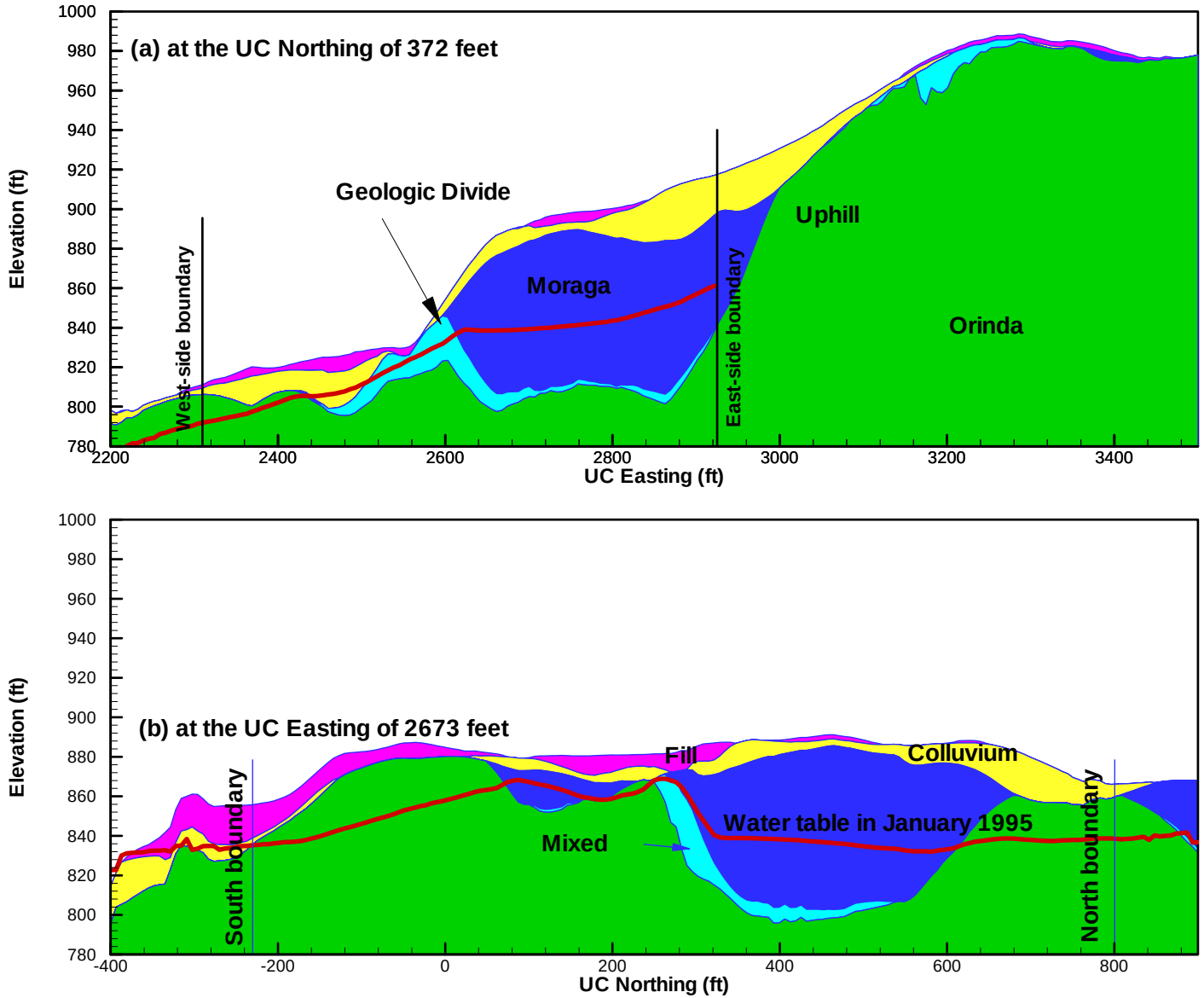

Figure 2. Geological profiles in vertical cross sections (a) in the UC Easting direction and (b) in the UC Northing direction, with representative water table.

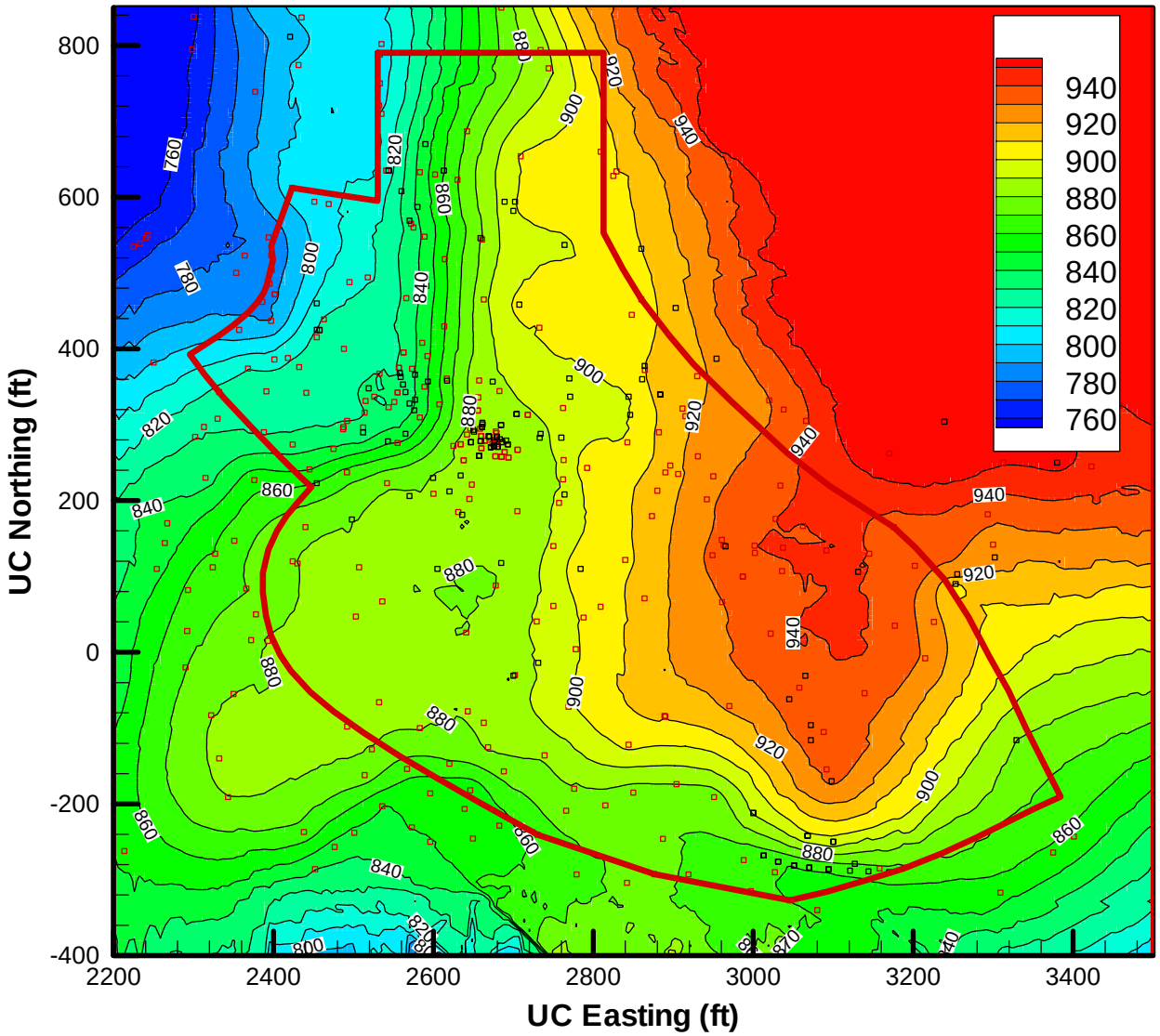

Figure 3. Surface elevation contours (ft) (the top of the Artificial Fill unit). Red squares indicate “full” boreholes and black squares indicate “partial” boreholes.

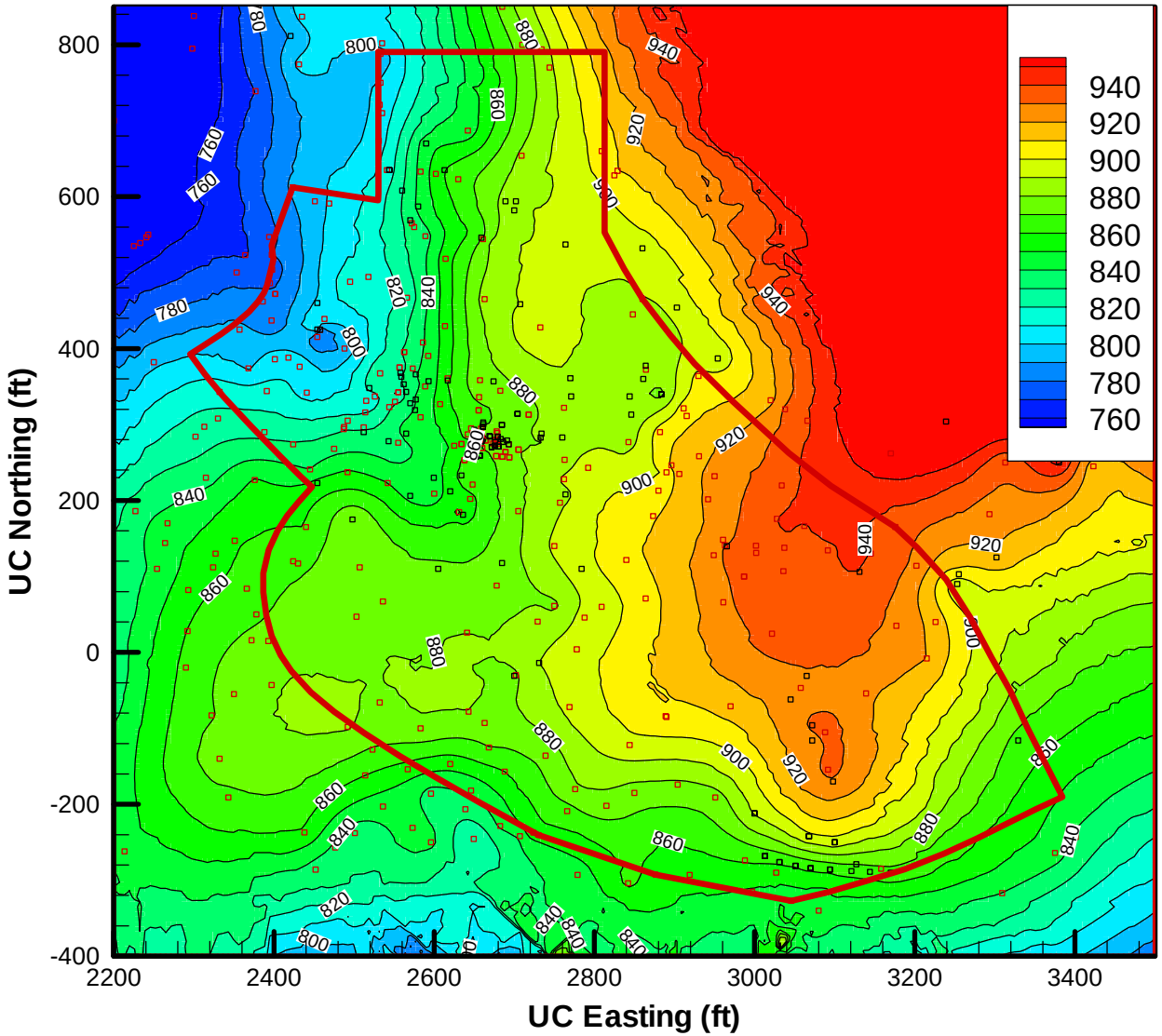

Figure 4. Structural contours of the top elevation (ft) of the Moraga Formation unit. Red squares indicate “full” boreholes and black squares indicate “partial” boreholes.

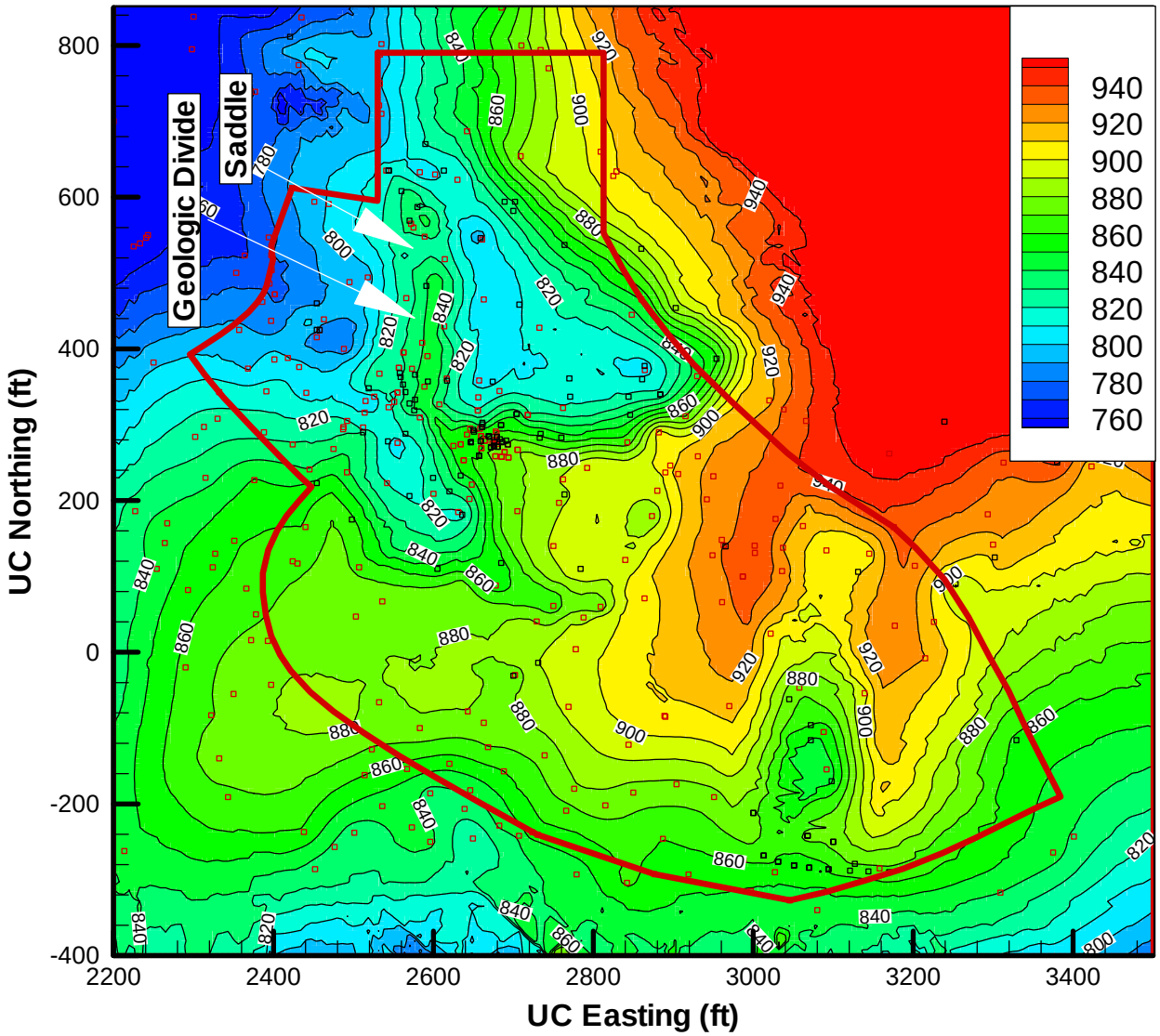

Figure 5. Structure contours of the top elevation (ft) of the Mixed unit. Red squares indicate “full” boreholes and black squares indicate “partial” boreholes.

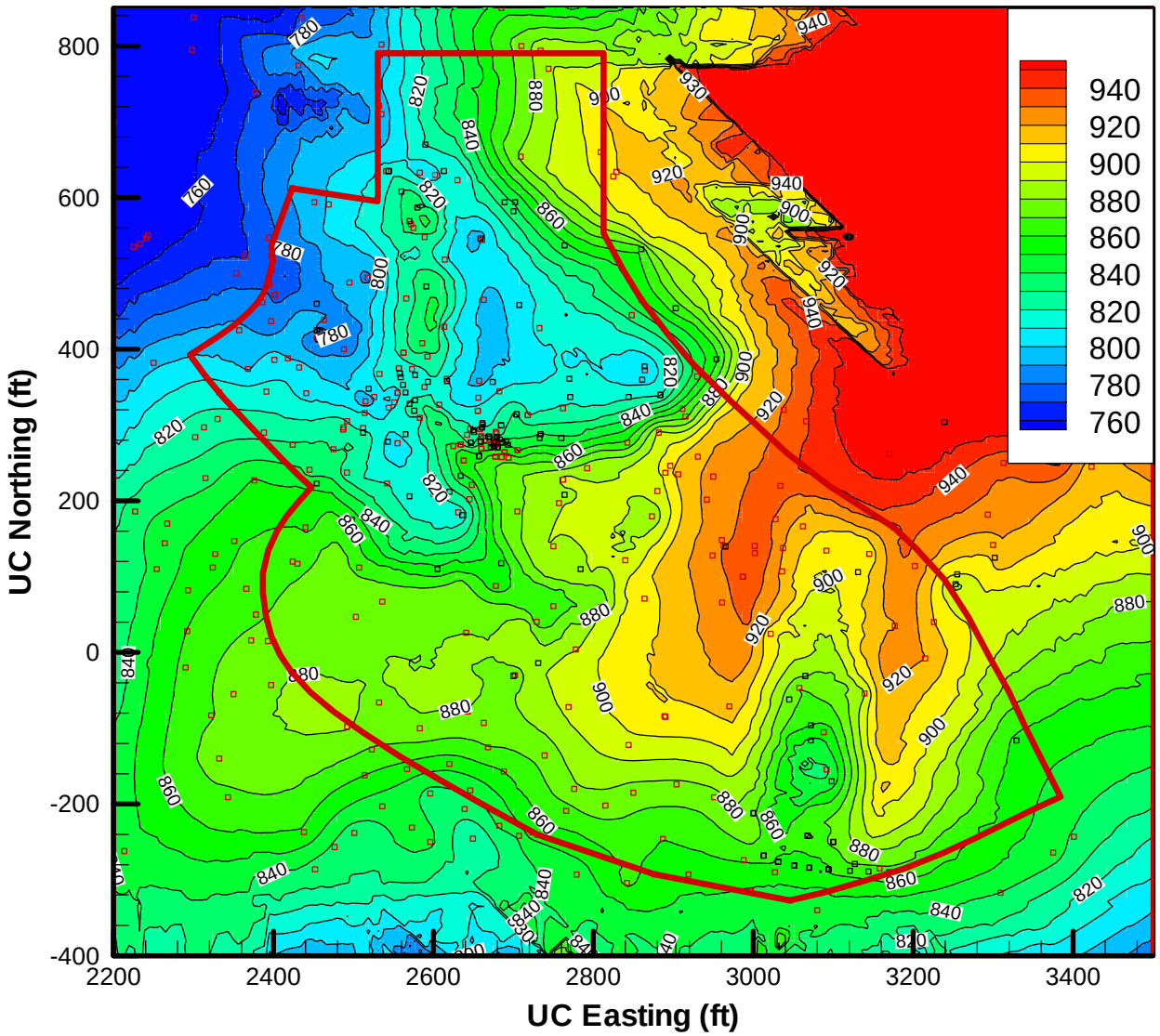

Figure 6. Structure contours of the top elevation (ft) of the Orinda Formation. Red squares indicate “full” boreholes and black squares indicate the interpolated top of the Orinda Formation for “partial” boreholes. Note that poor quality of interpolation can be seen in the east of the model domain.

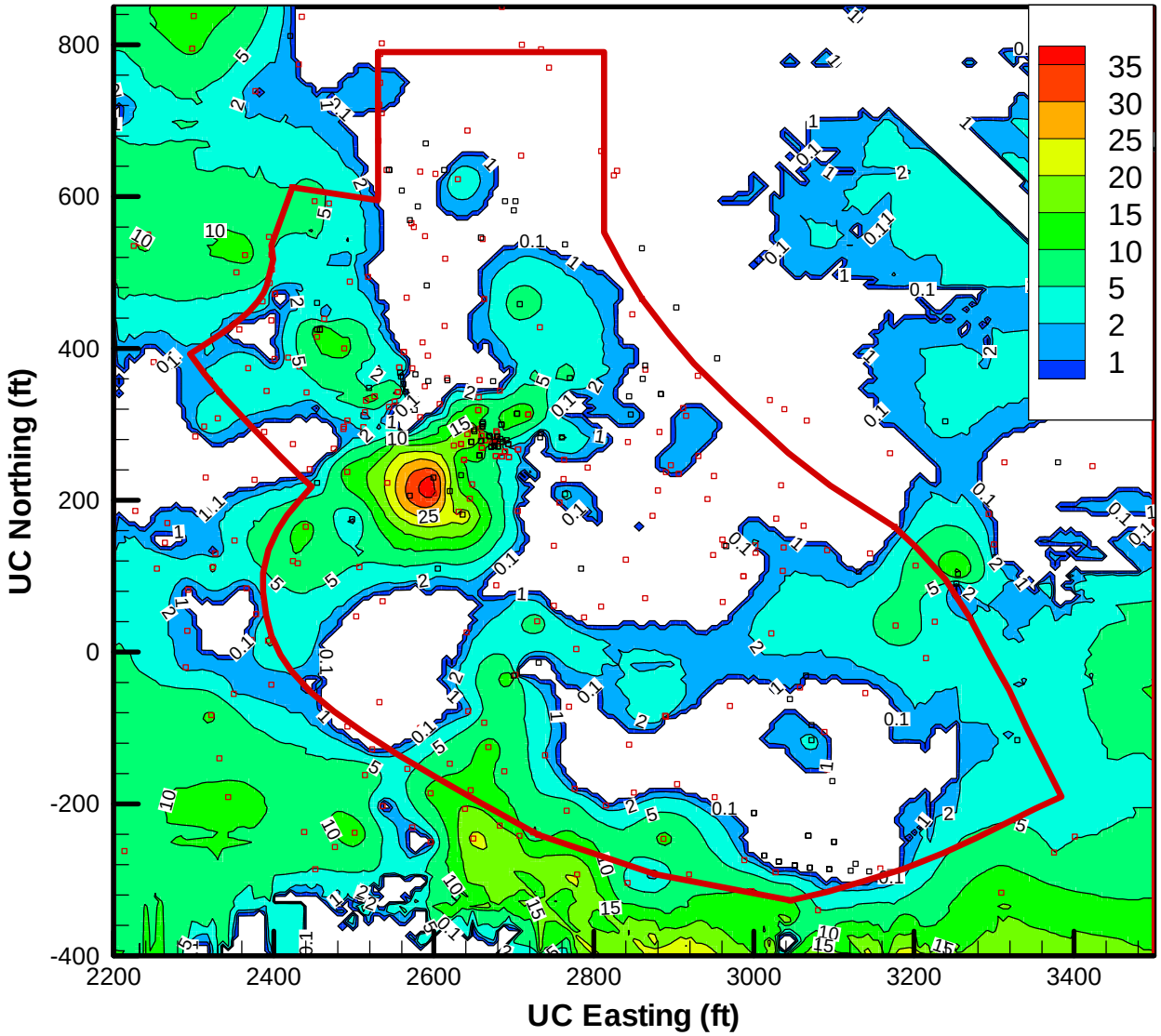

Figure 7. Thickness contours (ft) of the Artificial Fill unit. Red squares indicate “full” boreholes and black squares indicate “partial” boreholes.

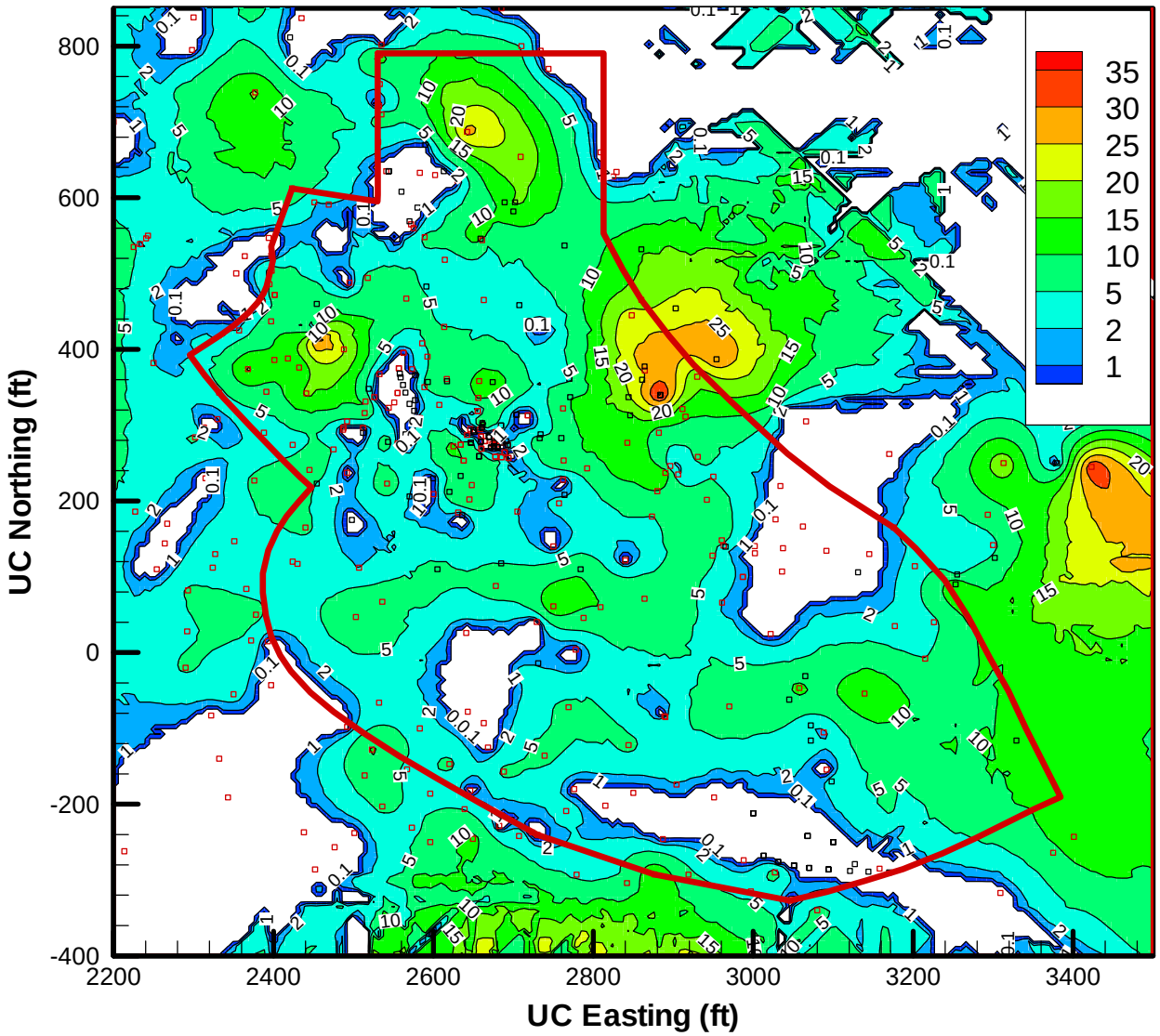

Figure 8. Thickness contours (ft) of the Colluvium unit. Red squares indicate “full” boreholes and black squares indicate “partial” boreholes.

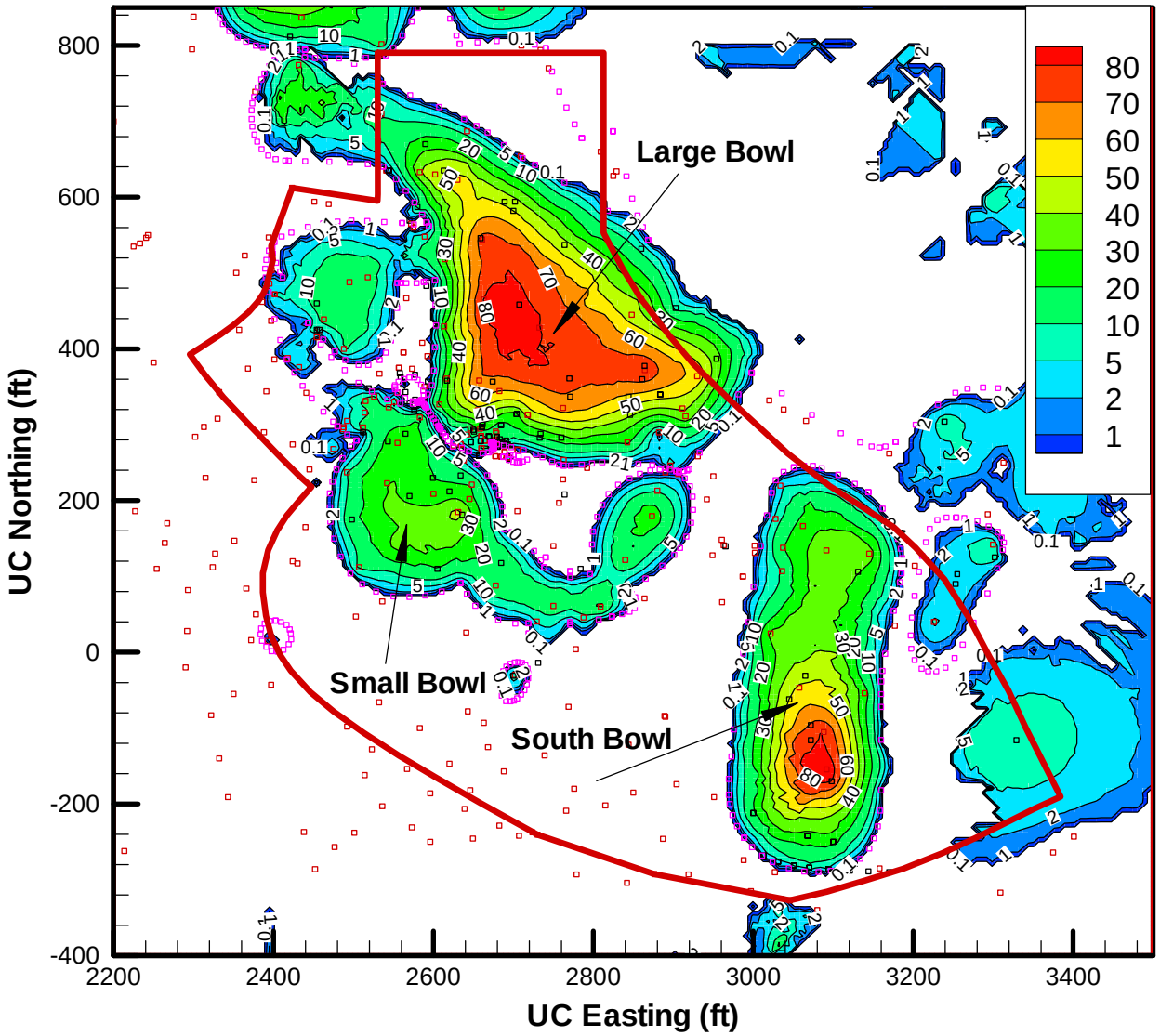

Figure 9. Thickness contours (ft) of the Moraga Formation unit. Red squares indicate “full” boreholes, black squares indicate “partial” boreholes, and purple squares indicate the zero-thickness data points obtained from the outcrop map.

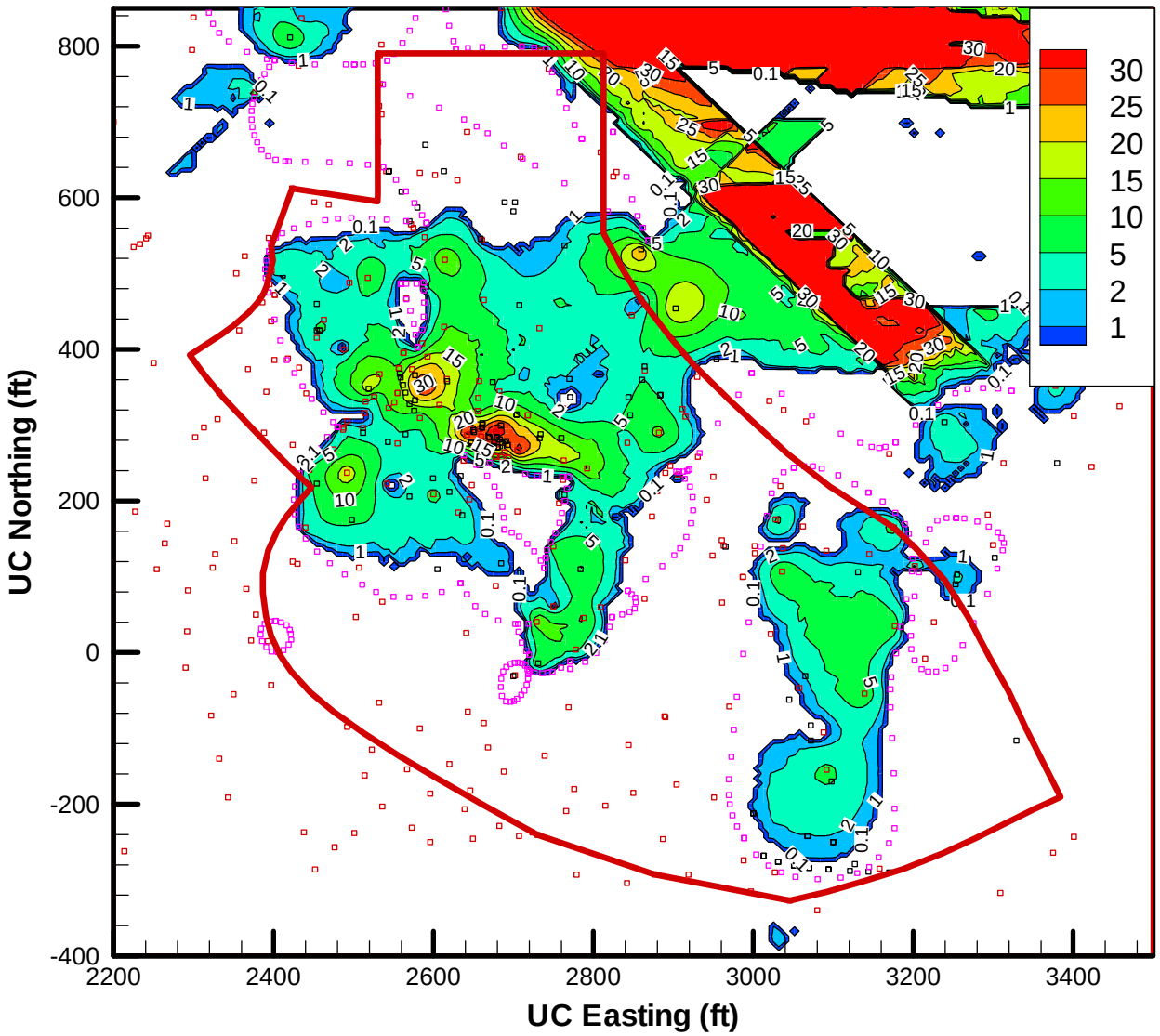

Figure 10. Thickness contours (ft) of the Mixed unit. Red squares indicate “full” boreholes, black squares indicate “partial” boreholes, and purple squares indicate the zero-thickness data points obtained from the outcrop map.

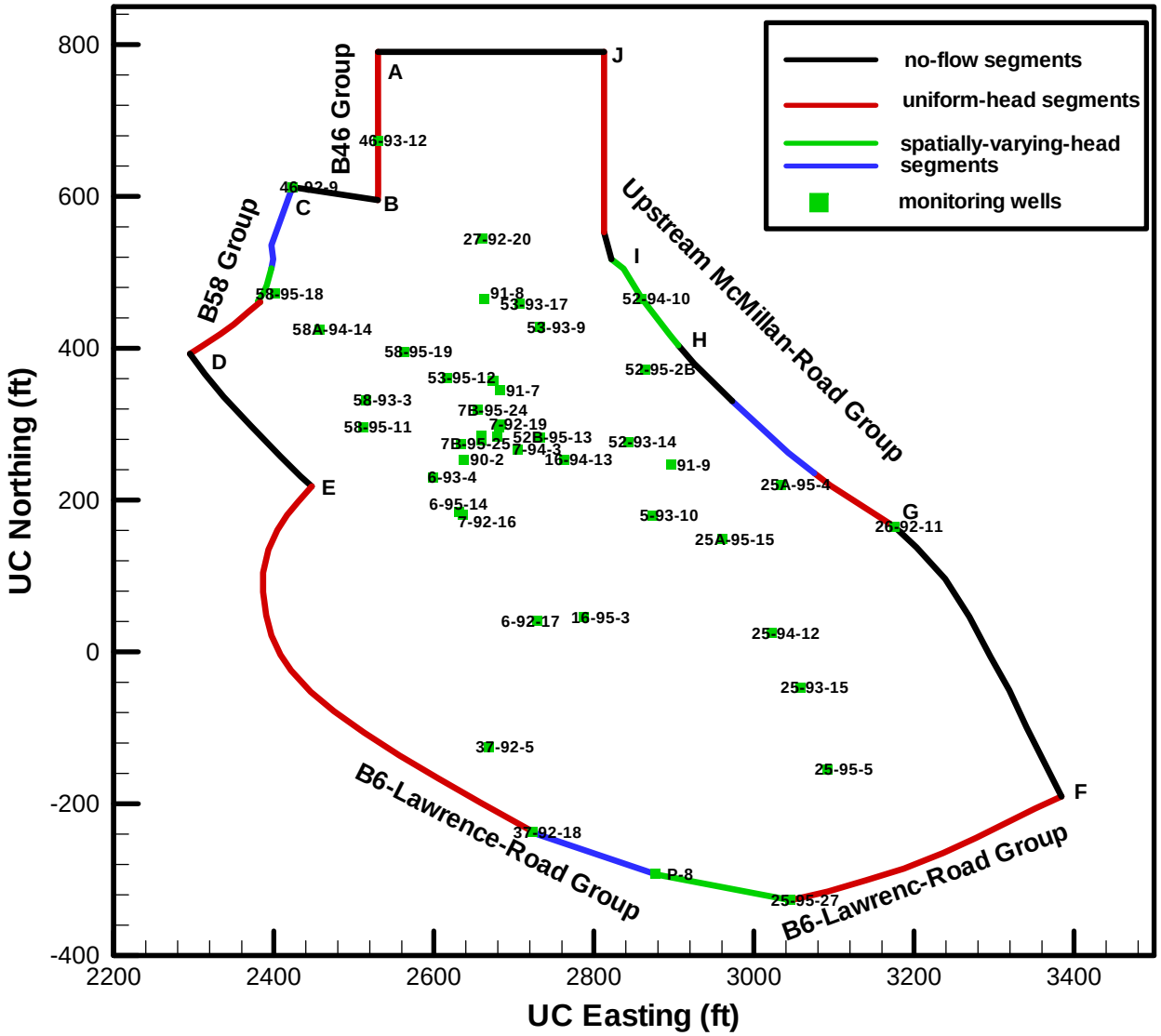

Figure 11. Model boundary, boundary condition types, boundary wells, and other monitoring wells used for determining initial conditions.

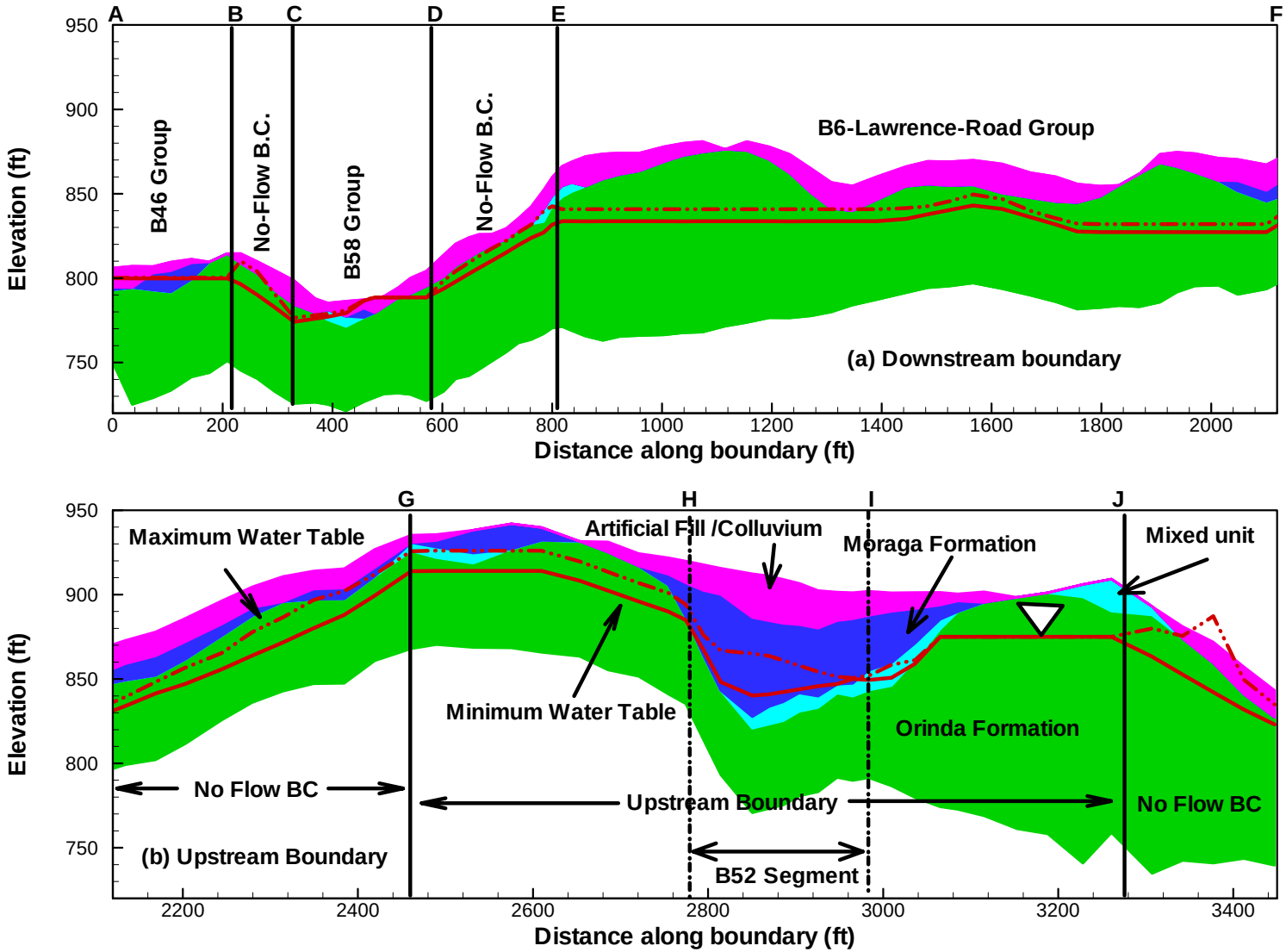

Figure 12. Geologic cross sections along the downstream and upstream boundaries of the model shown in Figure 11, with measured maximum and minimum water table specified on the boundary as boundary conditions.

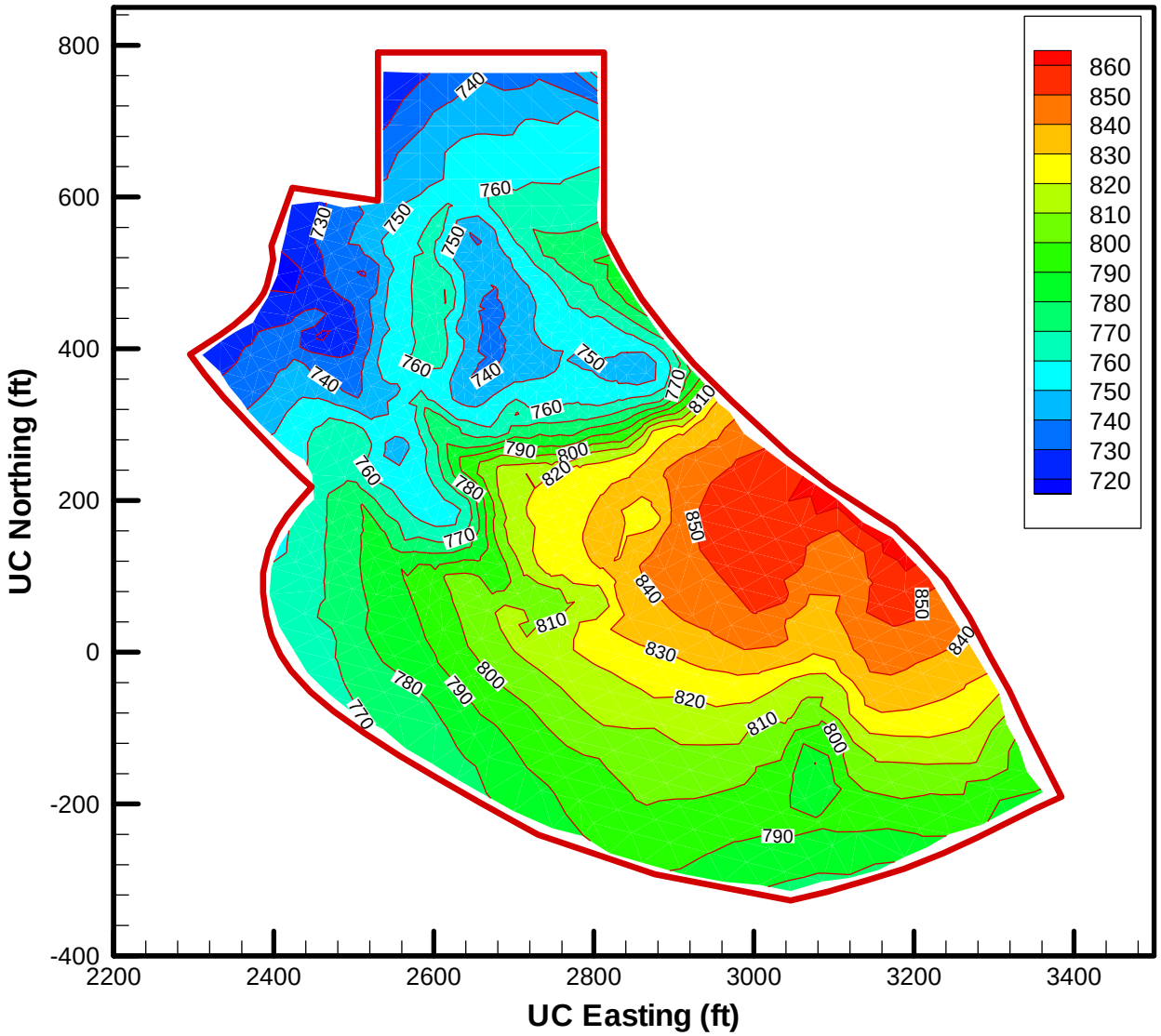

Figure 13. Elevation contours (ft) of model bottom boundary.

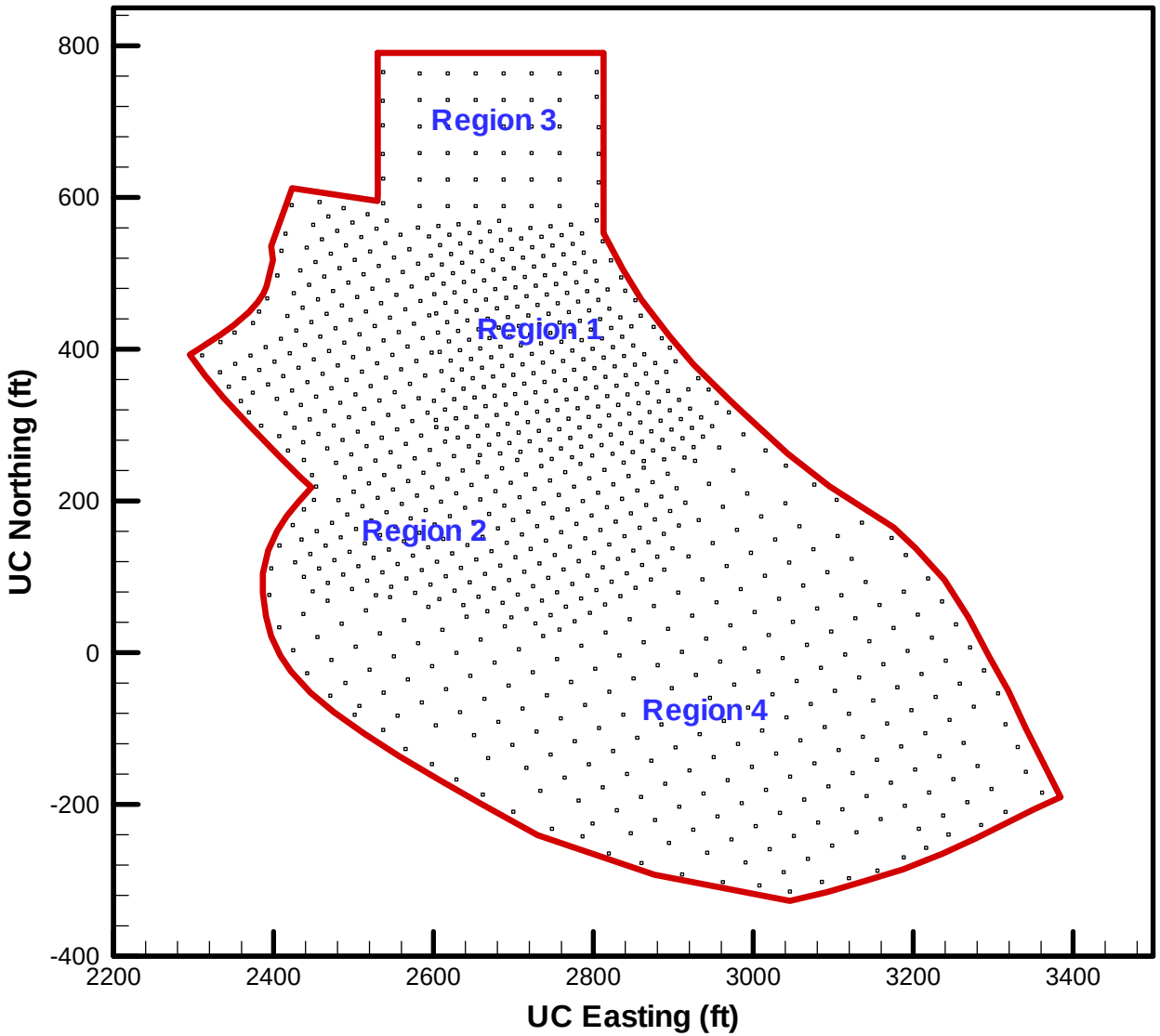

Figure 14. Plan view of the three-dimensional TOUGH2 grid for model calibration. Block dots are the centroids of vertical columns.

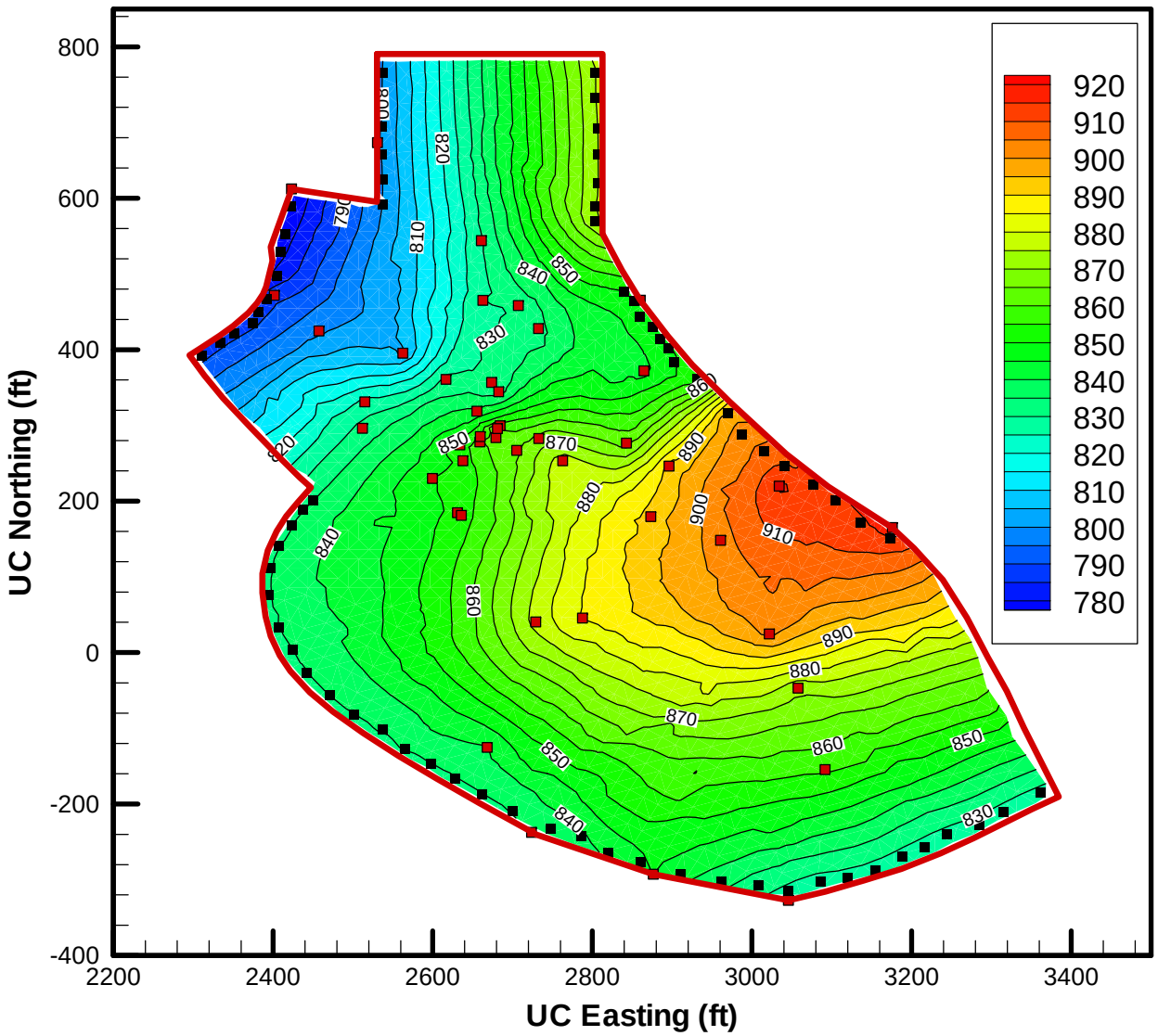

Figure 15. Elevation contours of the initial water table (ft) on June 30, 1994 obtained using the measured water levels at 47 monitoring wells (in red squares) and boundary conditions in boundary cells (in black squares).

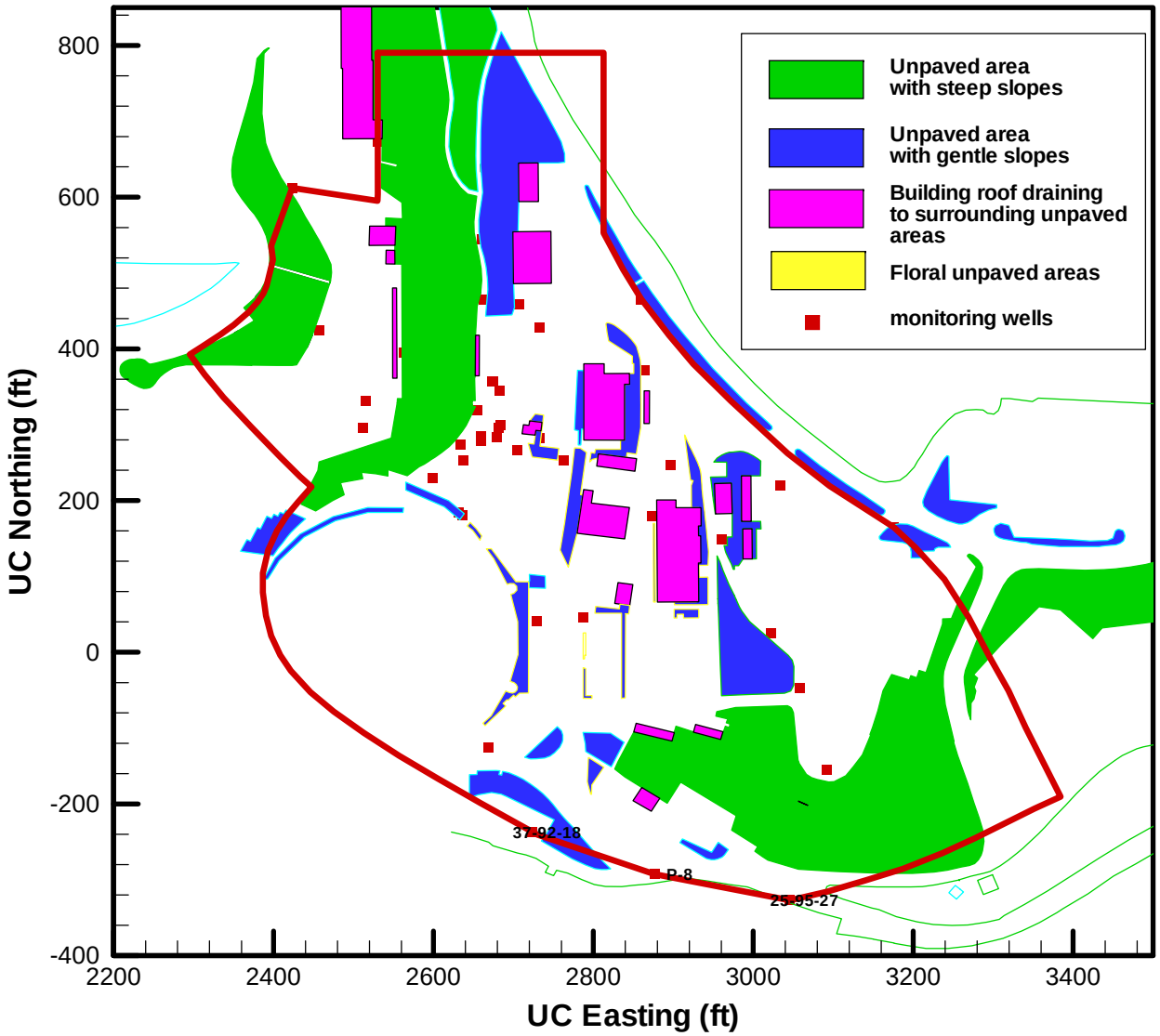

Figure 16. Map of the paved and unpaved areas for net recharge estimation. Green indicates the unpaved areas with steep slopes larger than 30°, whereas blue indicates those with gentle slopes. The purple areas are buildings with rainfall intercepted draining into neighboring unpaved areas.

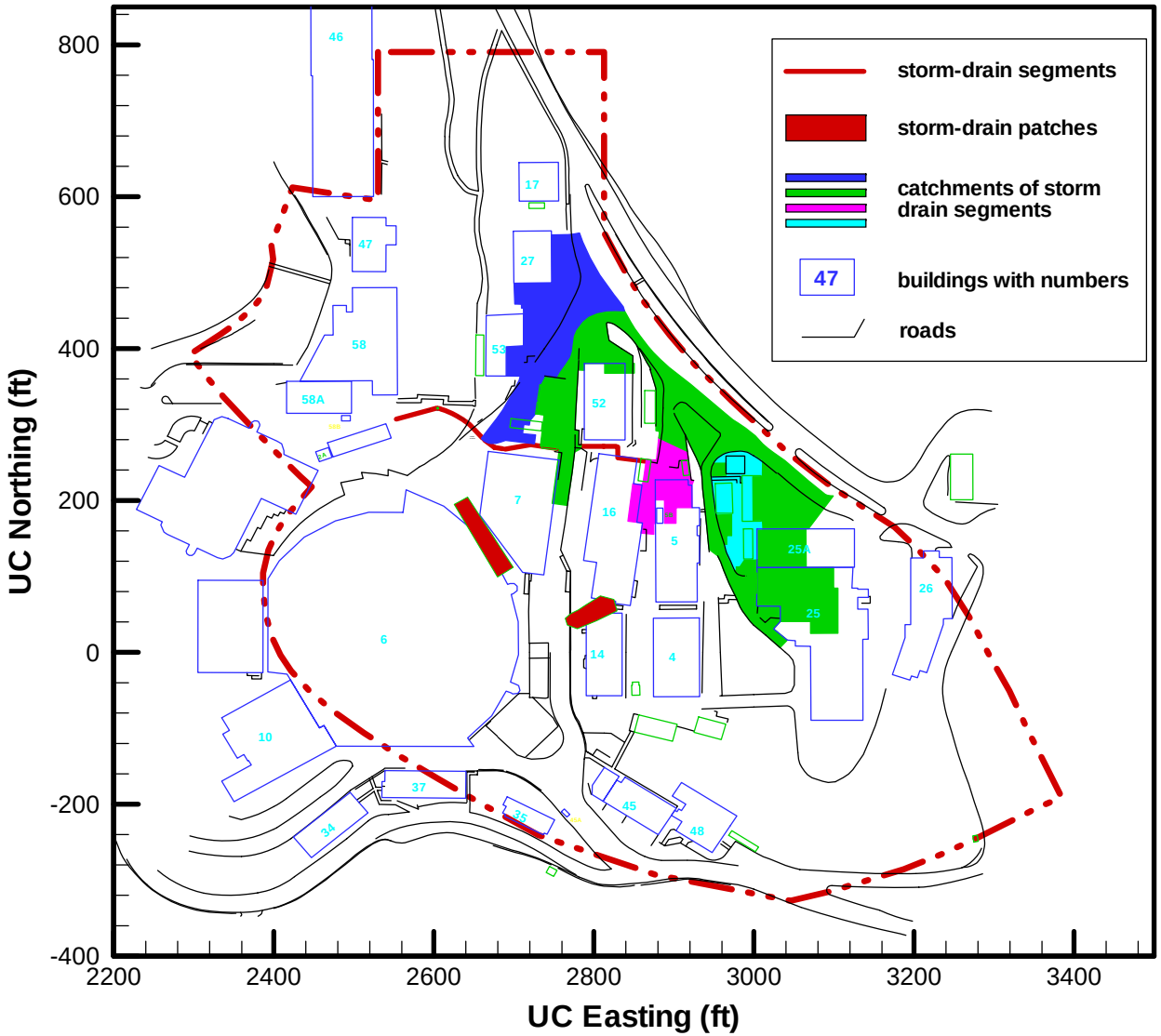

Figure 17. Confirmed leaking storm drains in red lines and patches and their discharge catchments. The main storm drain around Building 7 consists of four pipeline segments, each of which has a catchment for the discharging rainfall into pipeline. The storm drains in the north of Buildings 6 and 14 are in red patches.

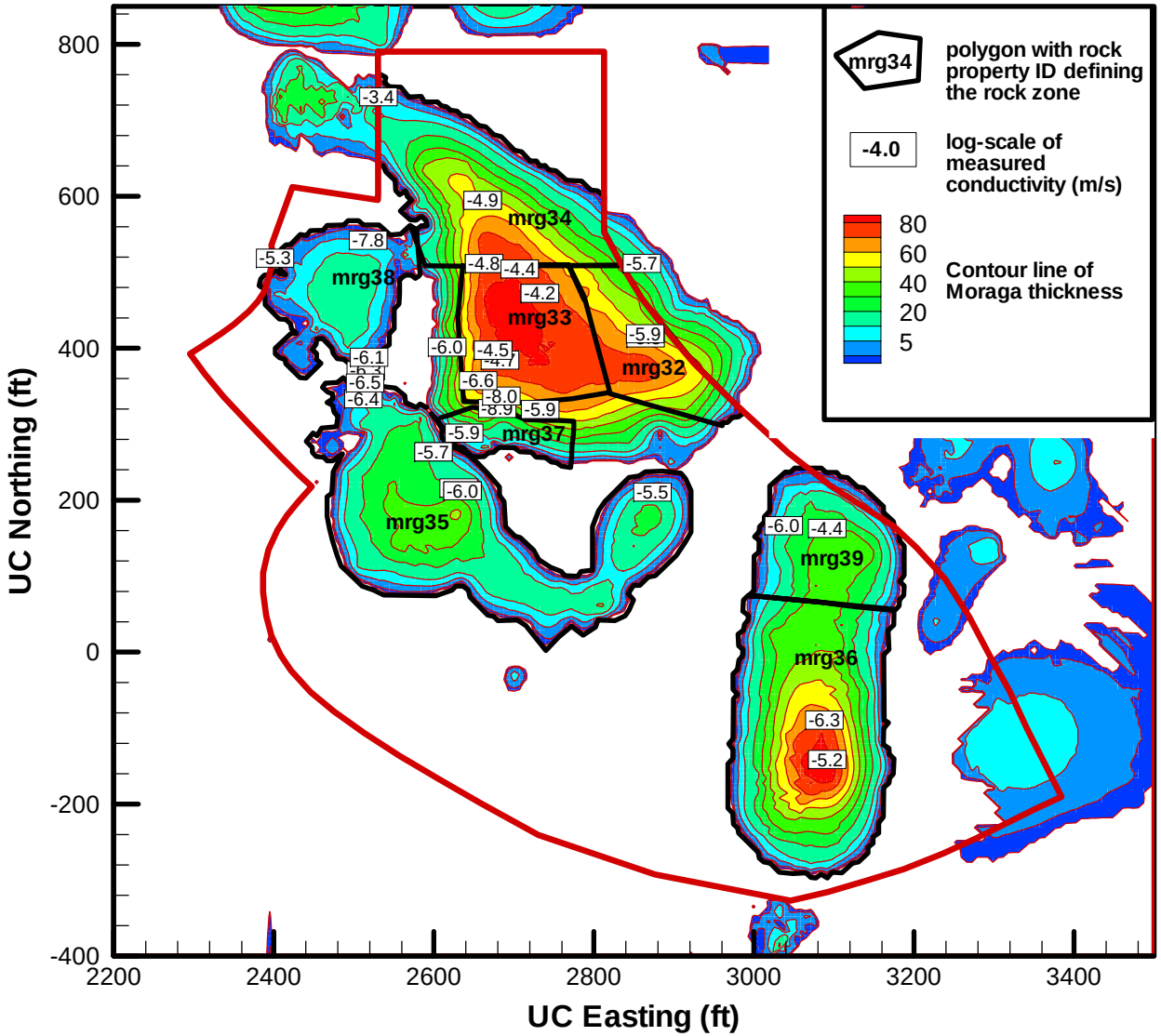

Figure 18. Definition of nine rock zones of different rock properties in the Moraga Formation unit, showing the measured hydraulic conductivities (m/s) in the log scale.

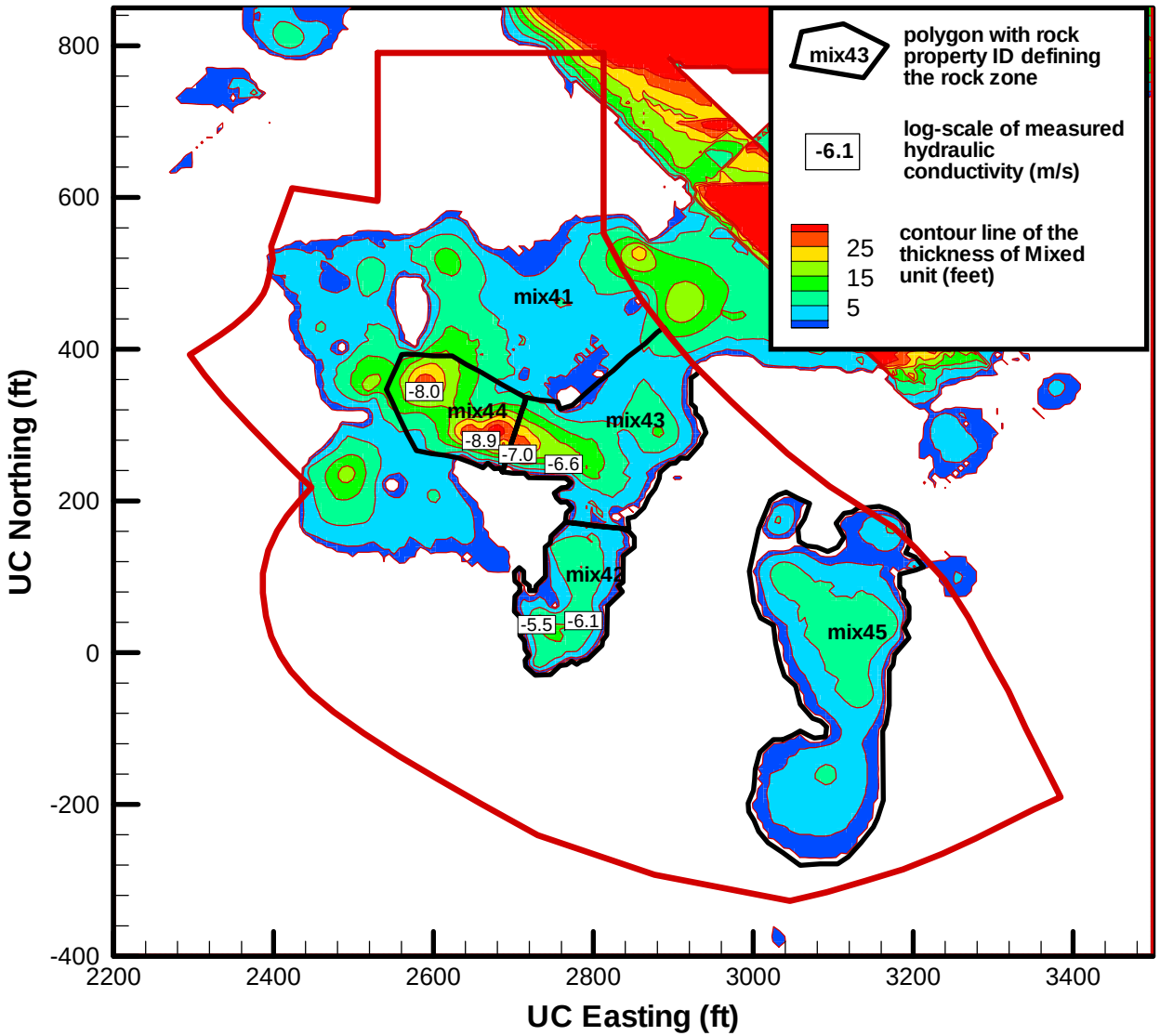

Figure 19. Definition of five rock zones of different rock properties in the Mixed unit, showing the measured hydraulic conductivities in the log scale.

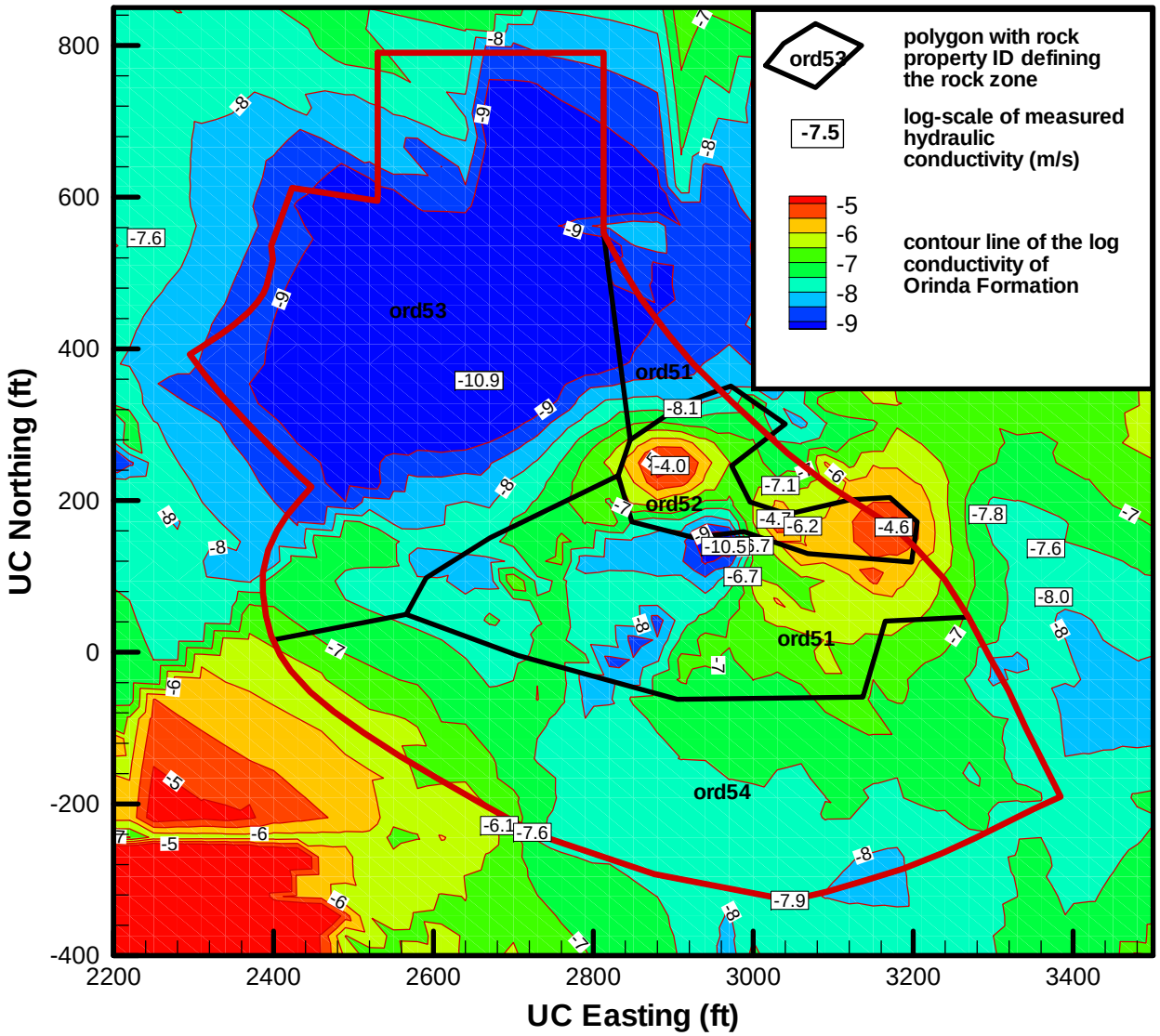

Figure 20. Definition of four rock zones of different rock properties in the Orinda Formation unit, showing the measured hydraulic conductivities in the log scale.

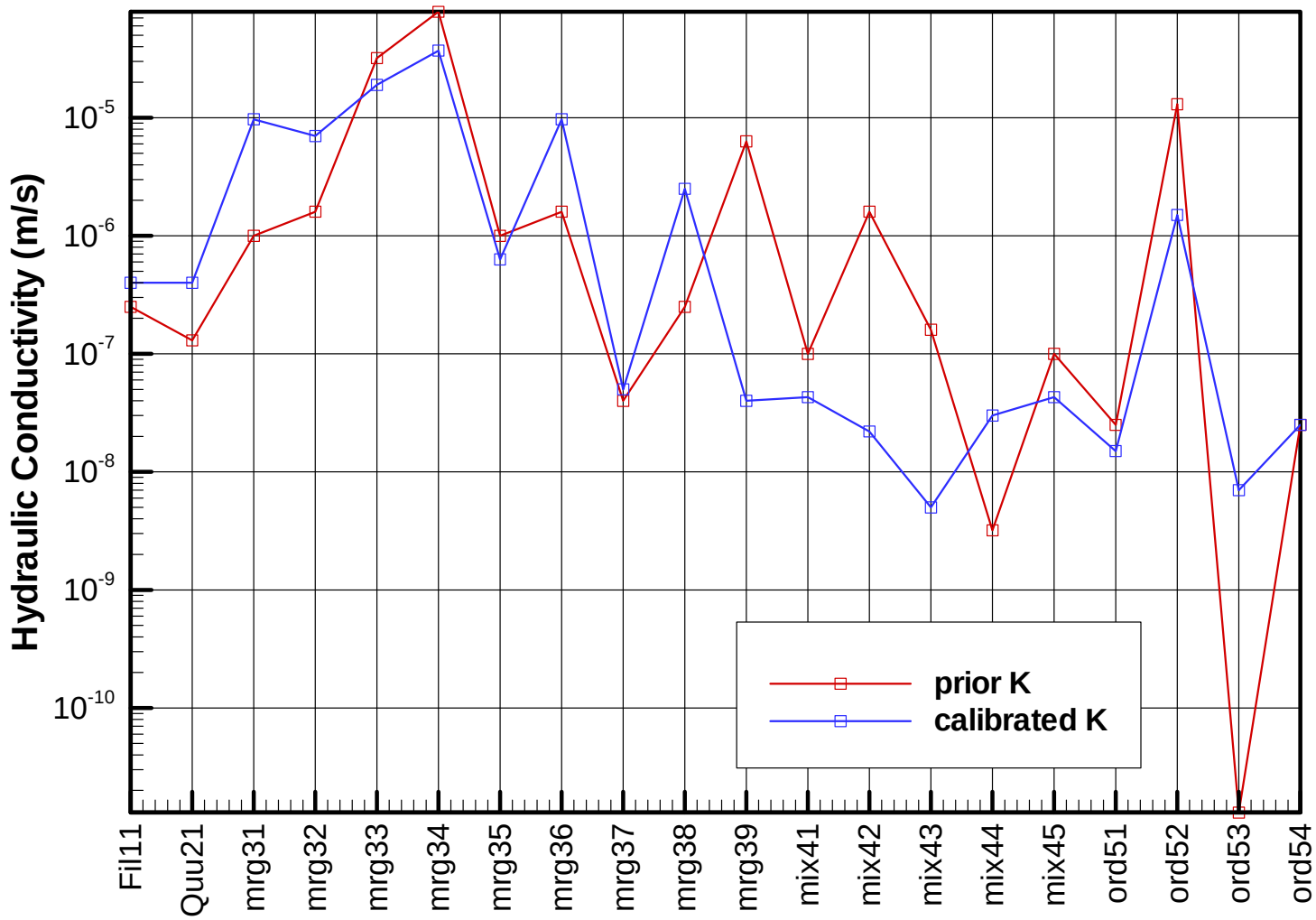

Figure 21. Comparison between the calibrated hydraulic conductivities and the prior ones obtained using hydraulic conductivity measurements for the 20 rock zones. See Figures 18-20 for the locations of the zones.

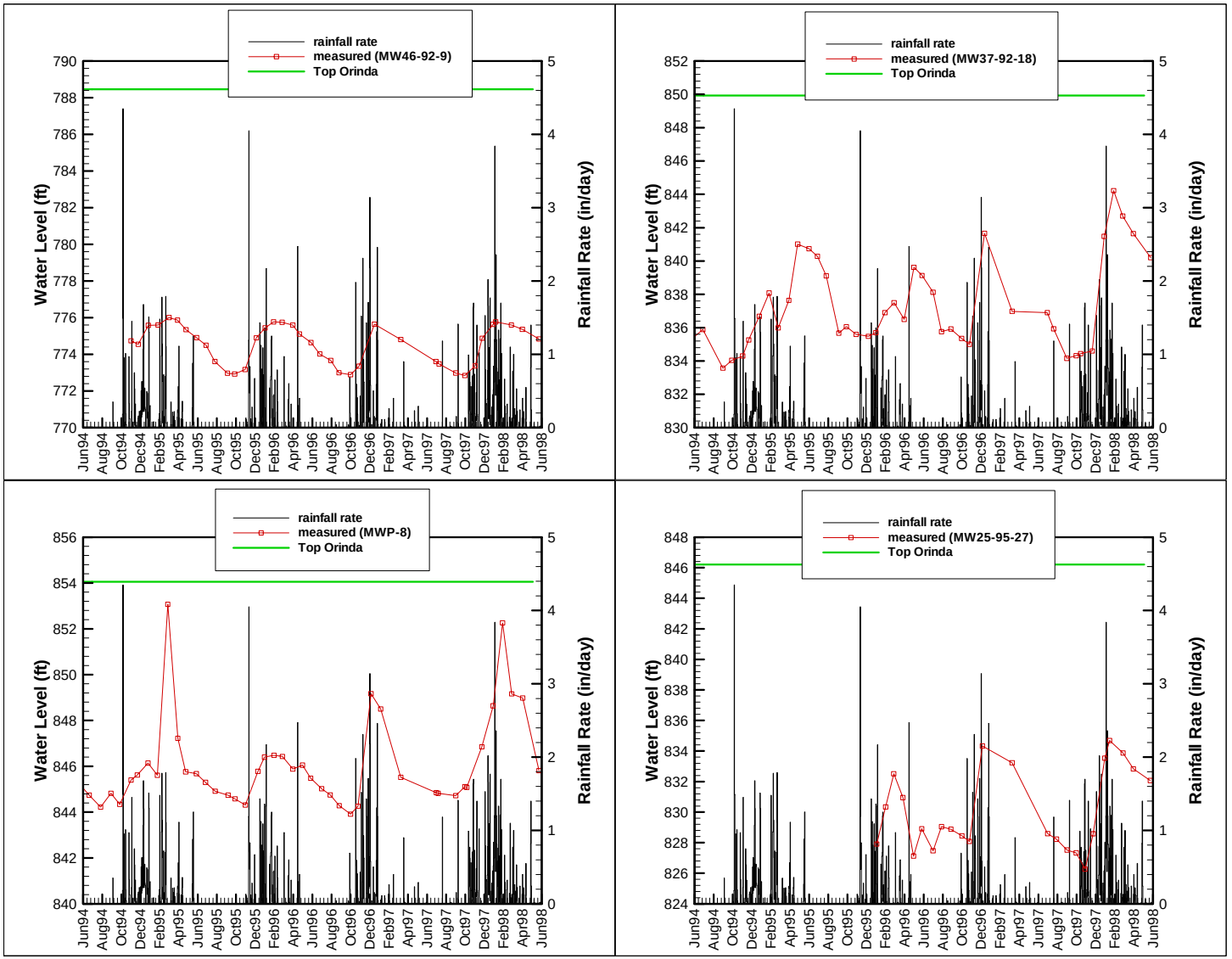

Figure 22. Measured water levels at four monitoring wells on the downstream boundary.

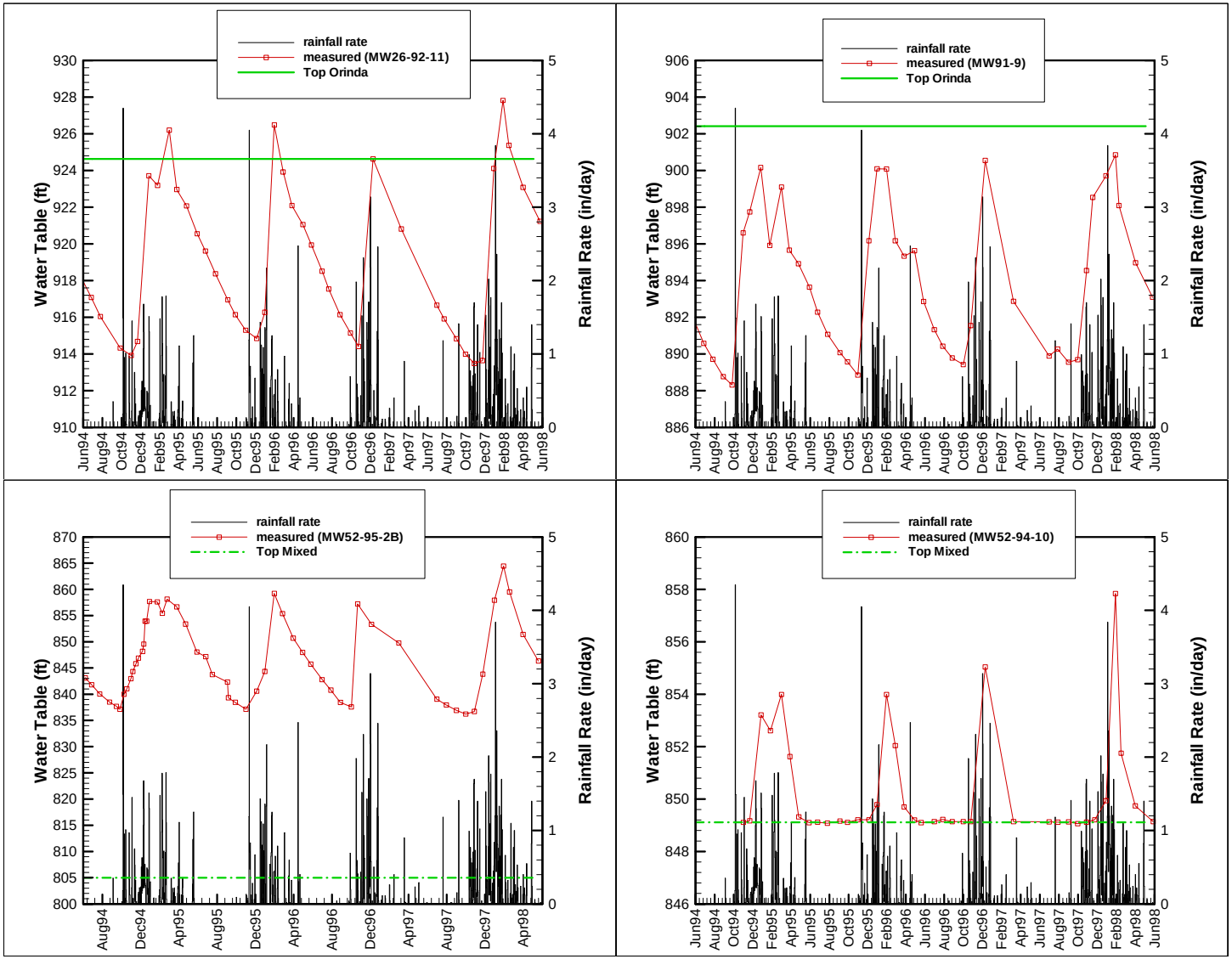

Figure 23. Measured water levels at four wells on the upstream boundary.

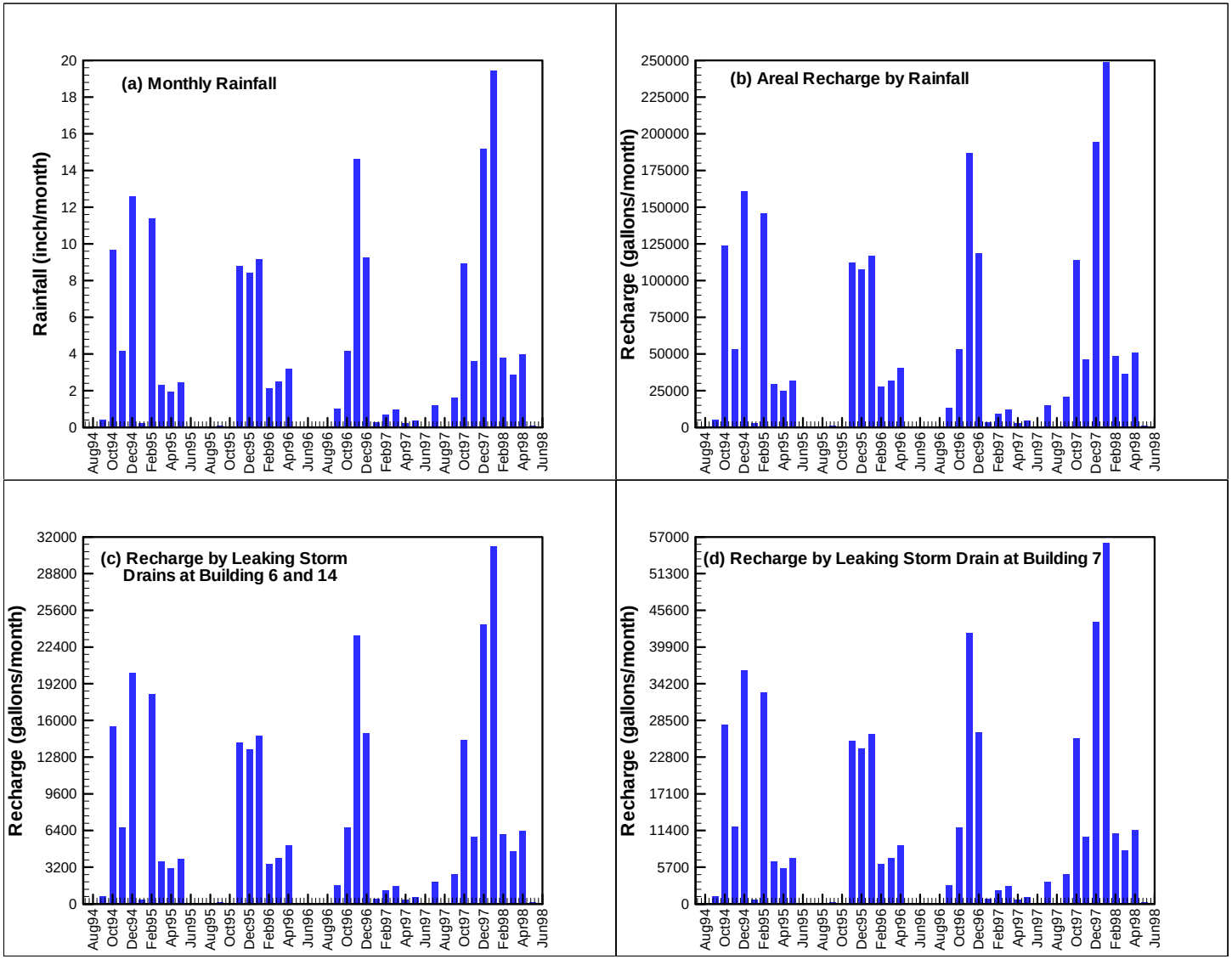

Figure 24. Transient processes of (a) monthly rainfall, (b) net areal recharge via unpaved areas, (c) recharge by storm drain at Building 6 and 14, and (d) recharge by storm drain in the north of Building 7 during the period from July 1994 to June 1998.

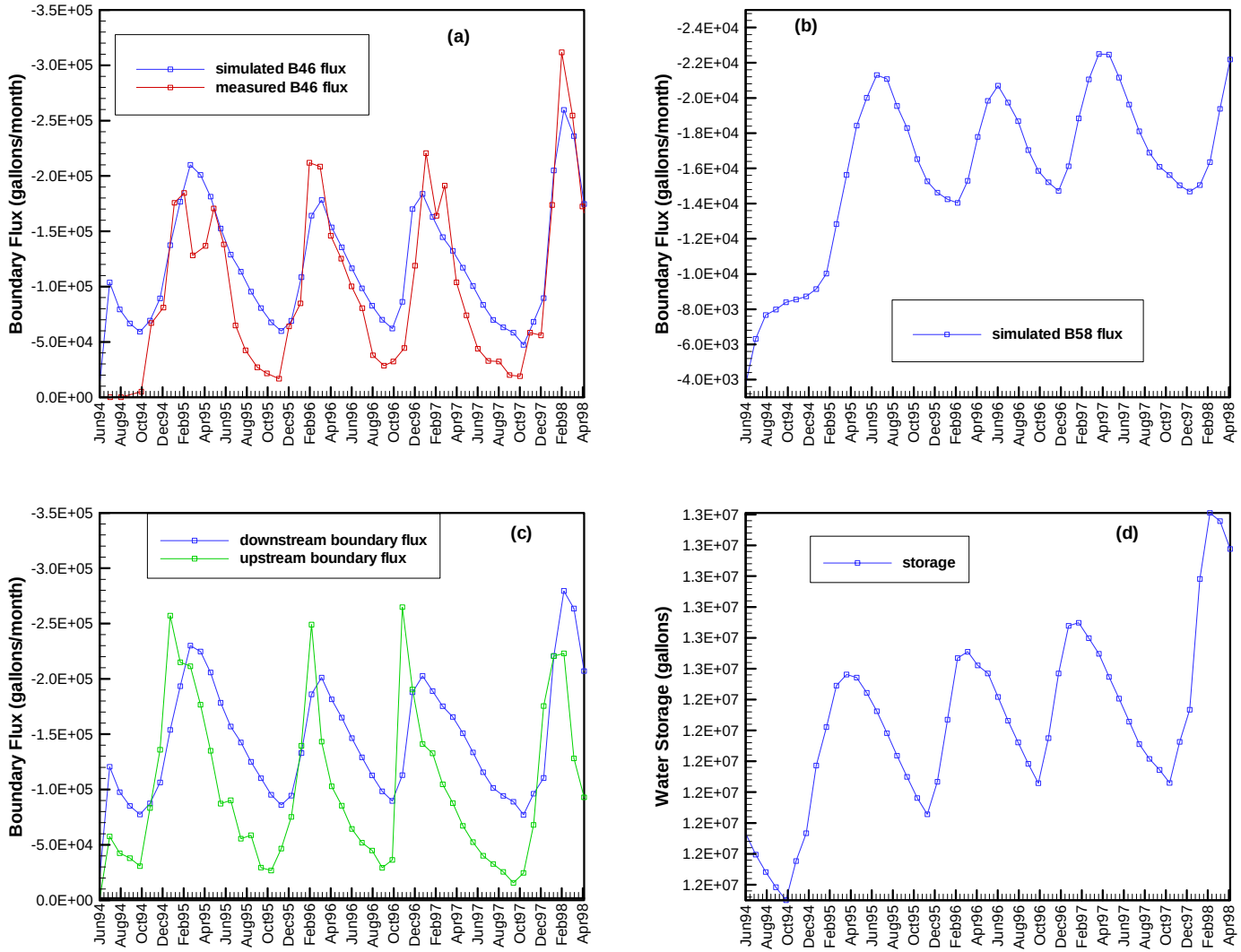

Figure 25. Transient processes of (a) the simulated and measured flow rate (gallons/month) through B46 boundary segment group, (b) the flow rate through B58 boundary segment group, (c) total inflow and outflow rates through the upstream boundary and downstream boundary, and (d) water-storage change (gallons) in the system during the period from July 1994 to June 1998.

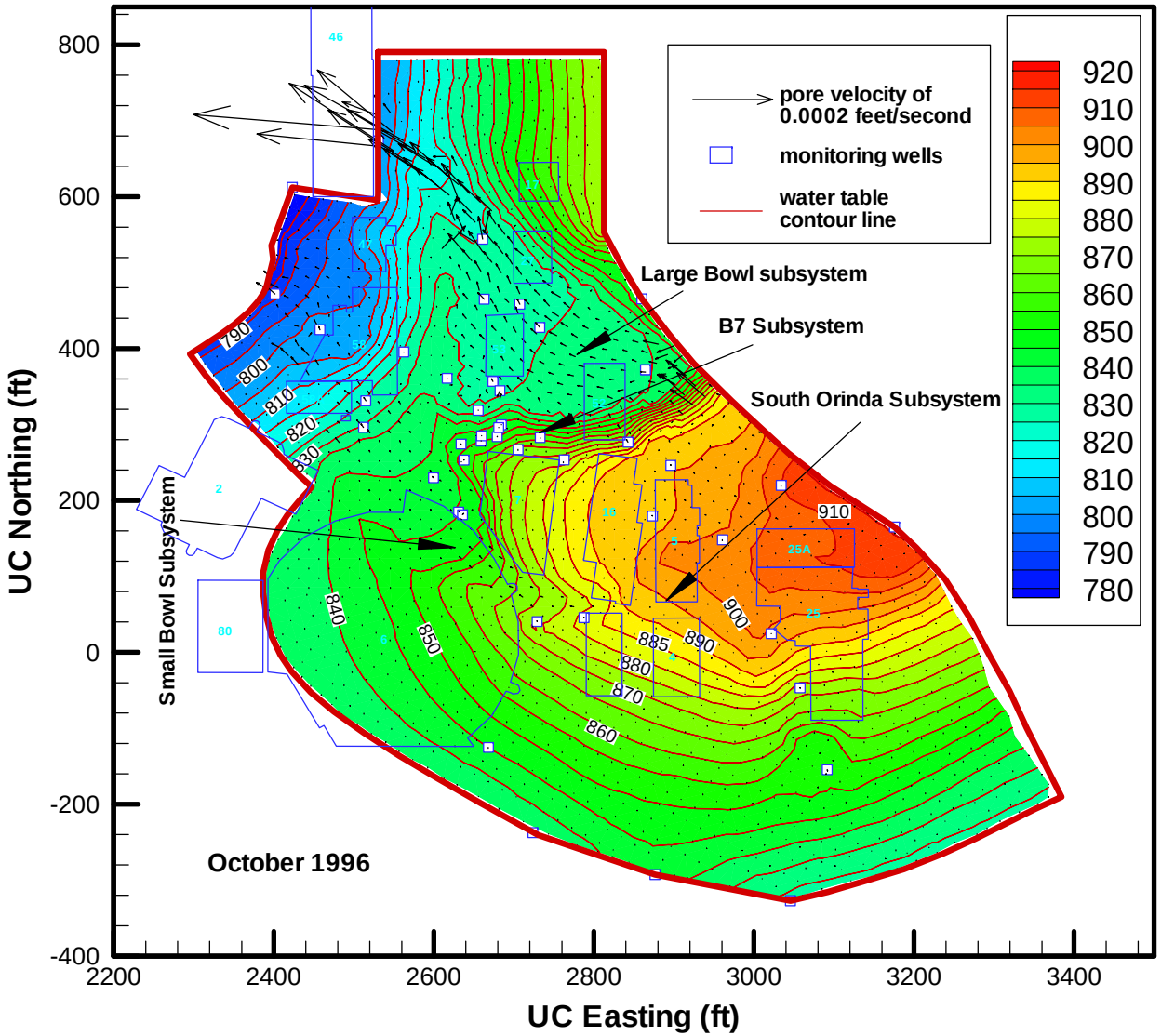

Figure 26. Contour of the simulated water table and vector field of simulated velocity on the water table at October 1996. The blue-white symbols indicate the location of monitoring wells.

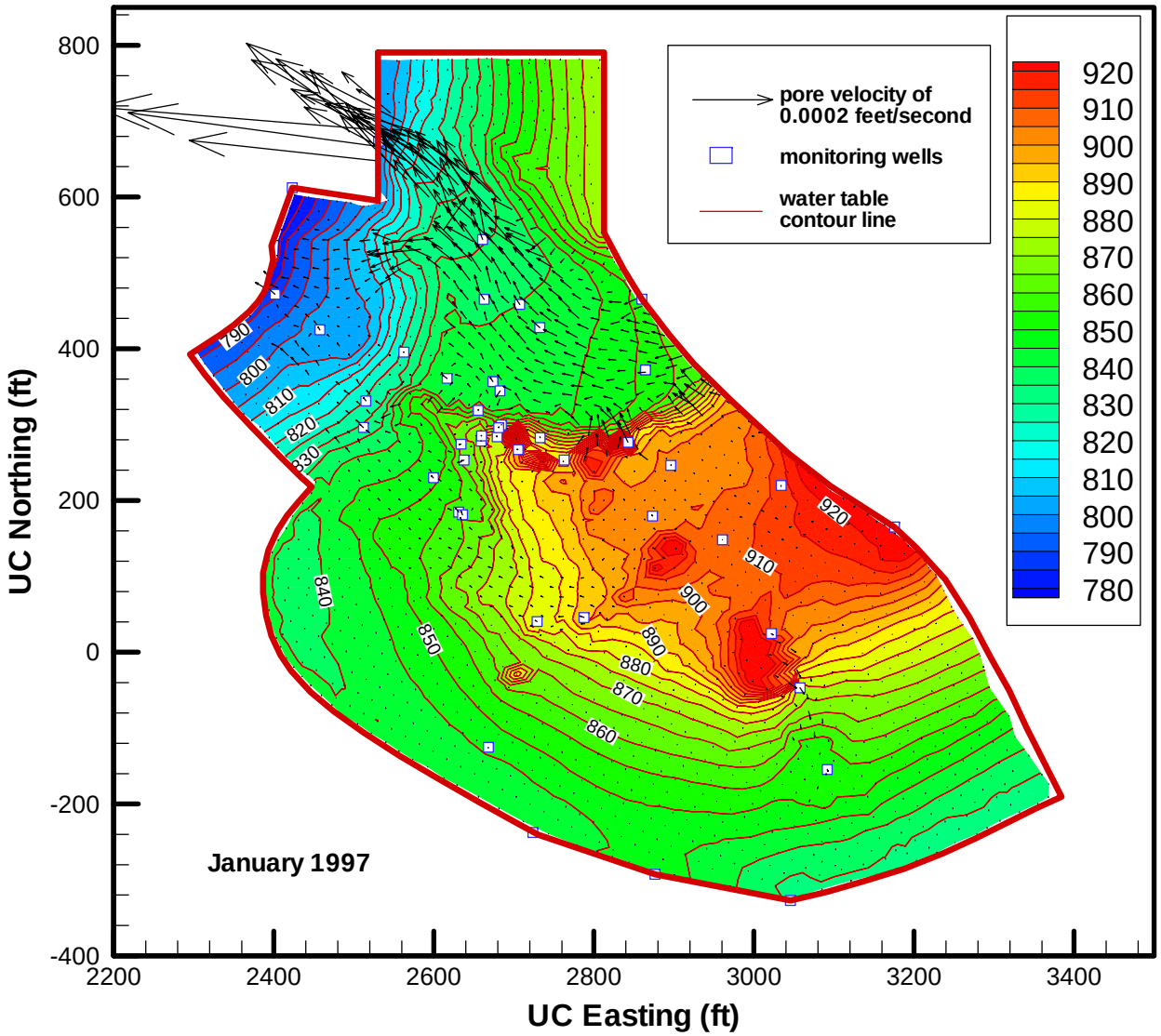

Figure 27. Contour of the simulated water table and vector field of simulated velocity on the water table at January 1997. The blue-white symbols indicate the location of monitoring wells.

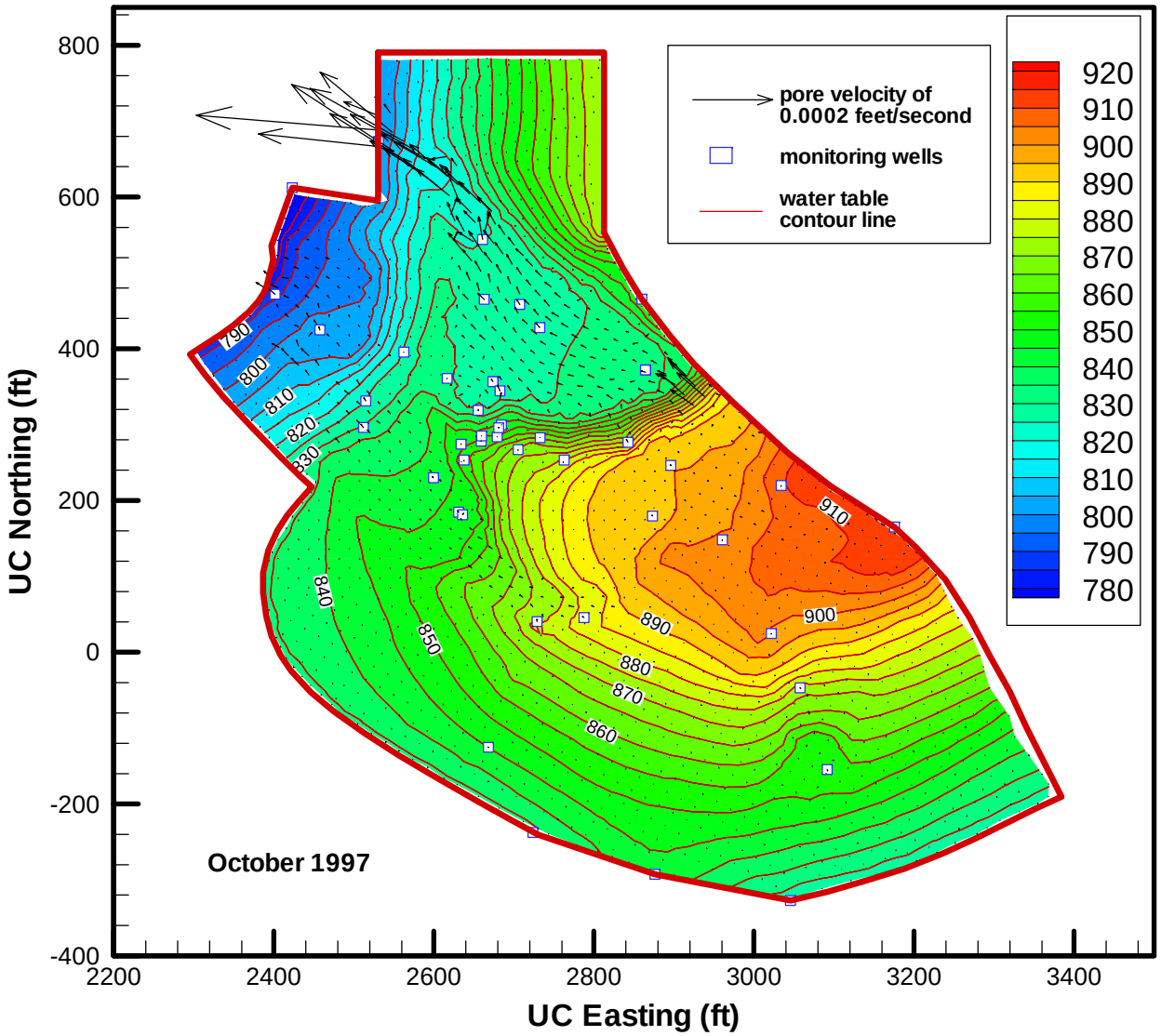

Figure 28. Contour of the simulated water table and vector field of simulated velocity on the water table at October 1997. The blue-white symbols indicate the location of monitoring wells.

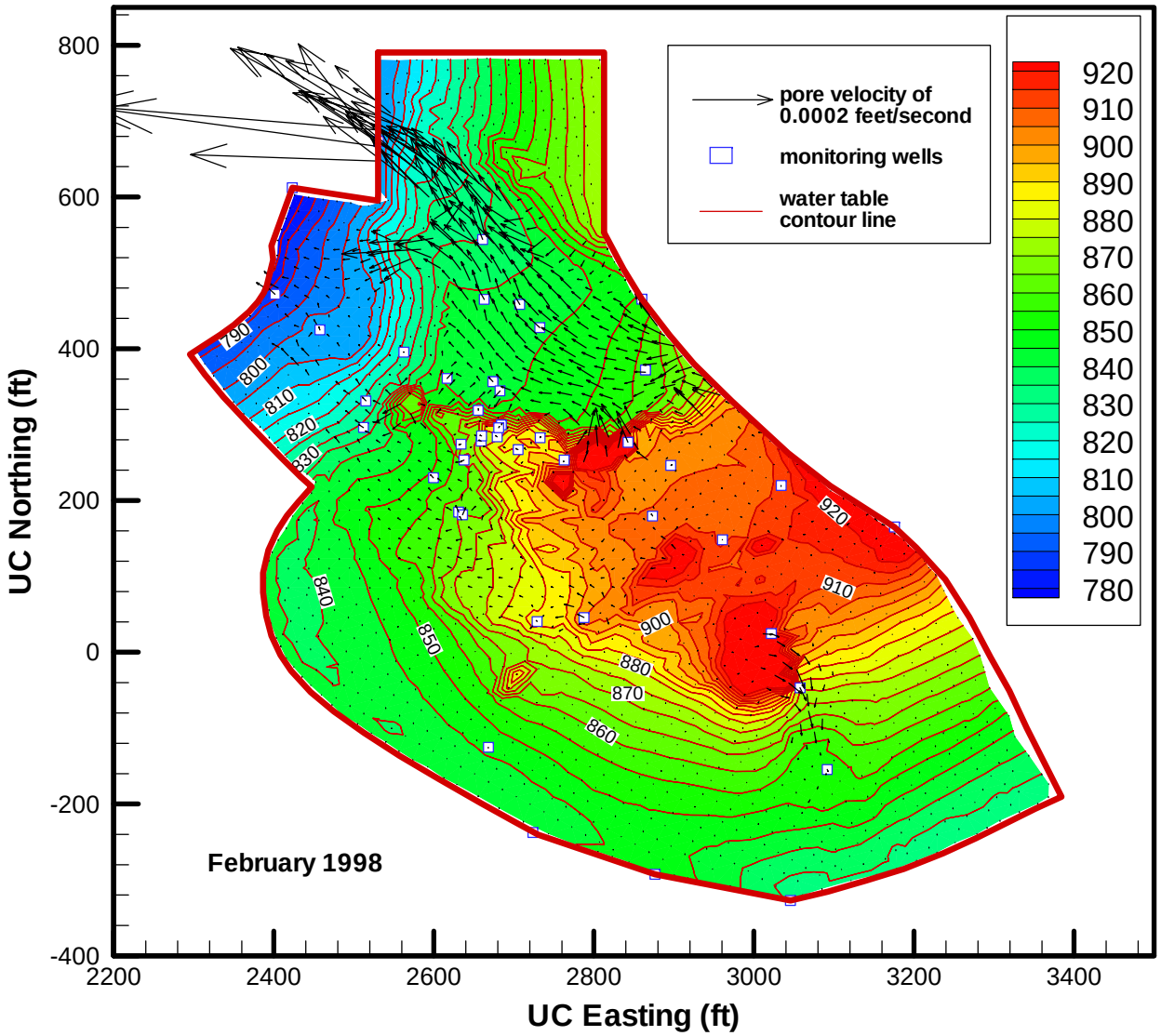

Figure 29. Contour of the simulated water table and vector field of simulated velocity on the water table at February 1998. The blue-white symbols indicate the location of monitoring wells.

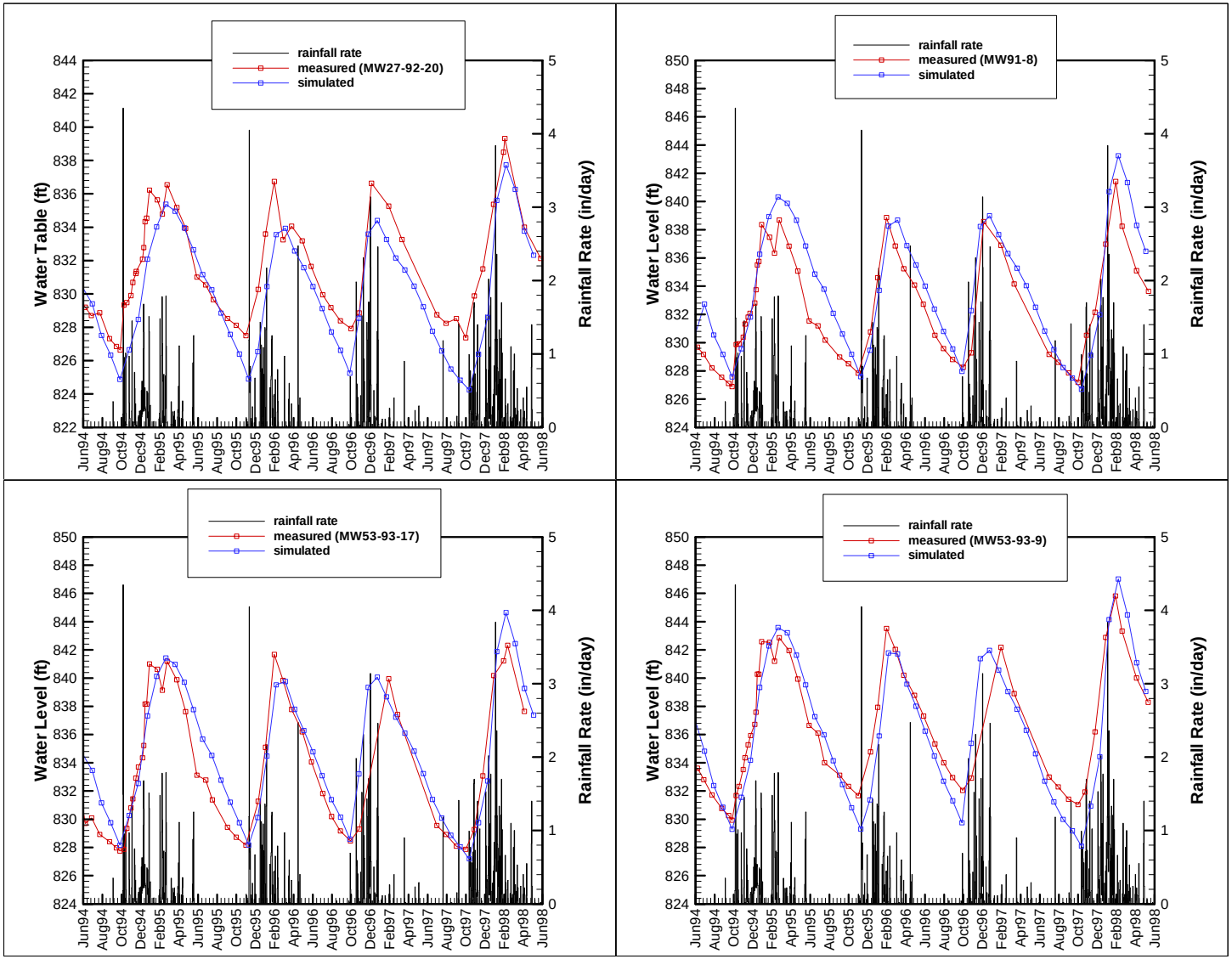

Figure 30. Match between the measured and simulated water levels at four monitoring wells in the Large-Moraga-Bowl subsystem.

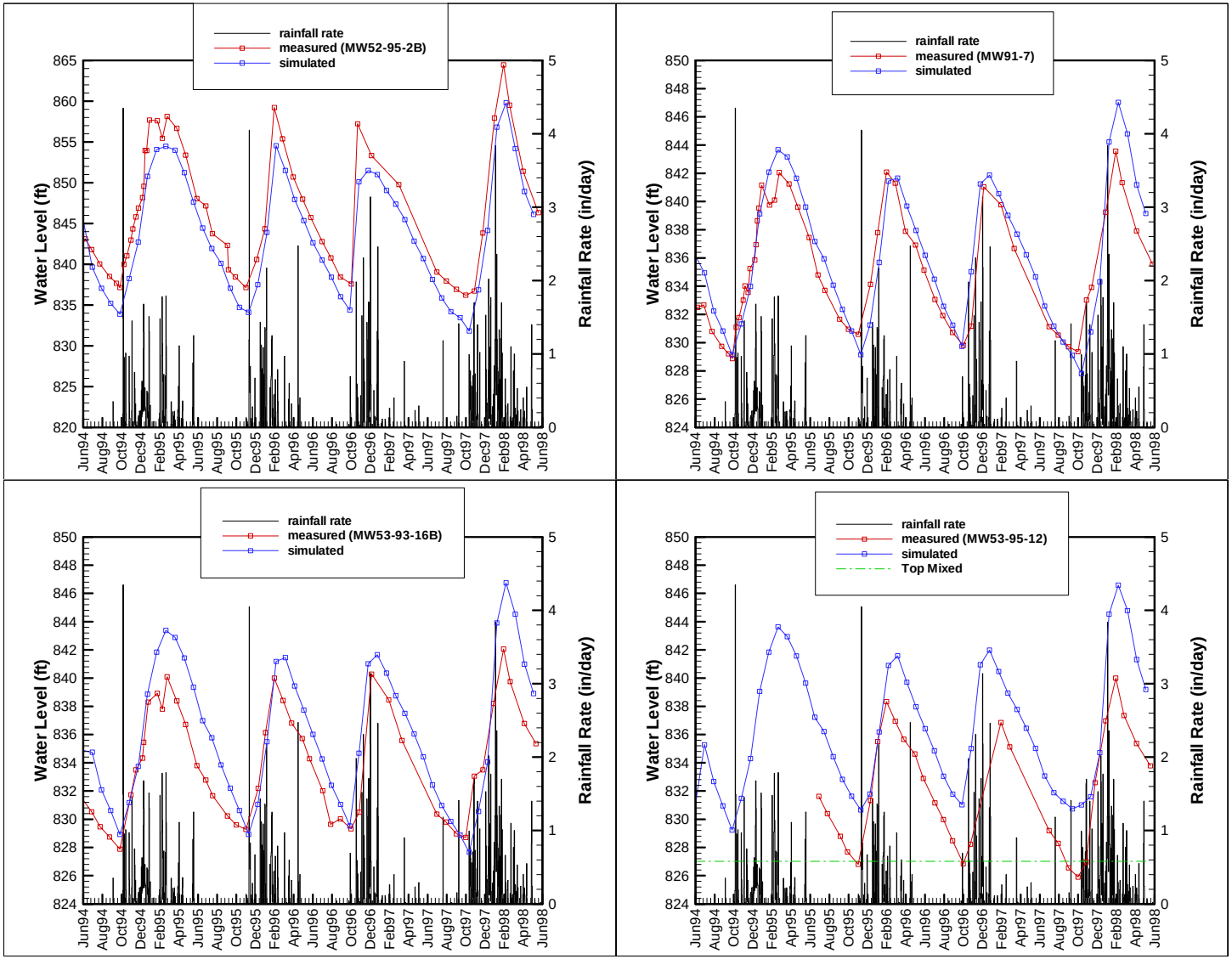

Figure 31. Match between the measured and simulated water levels at four monitoring wells in the Large-Moraga-Bowl subsystem (cont.).

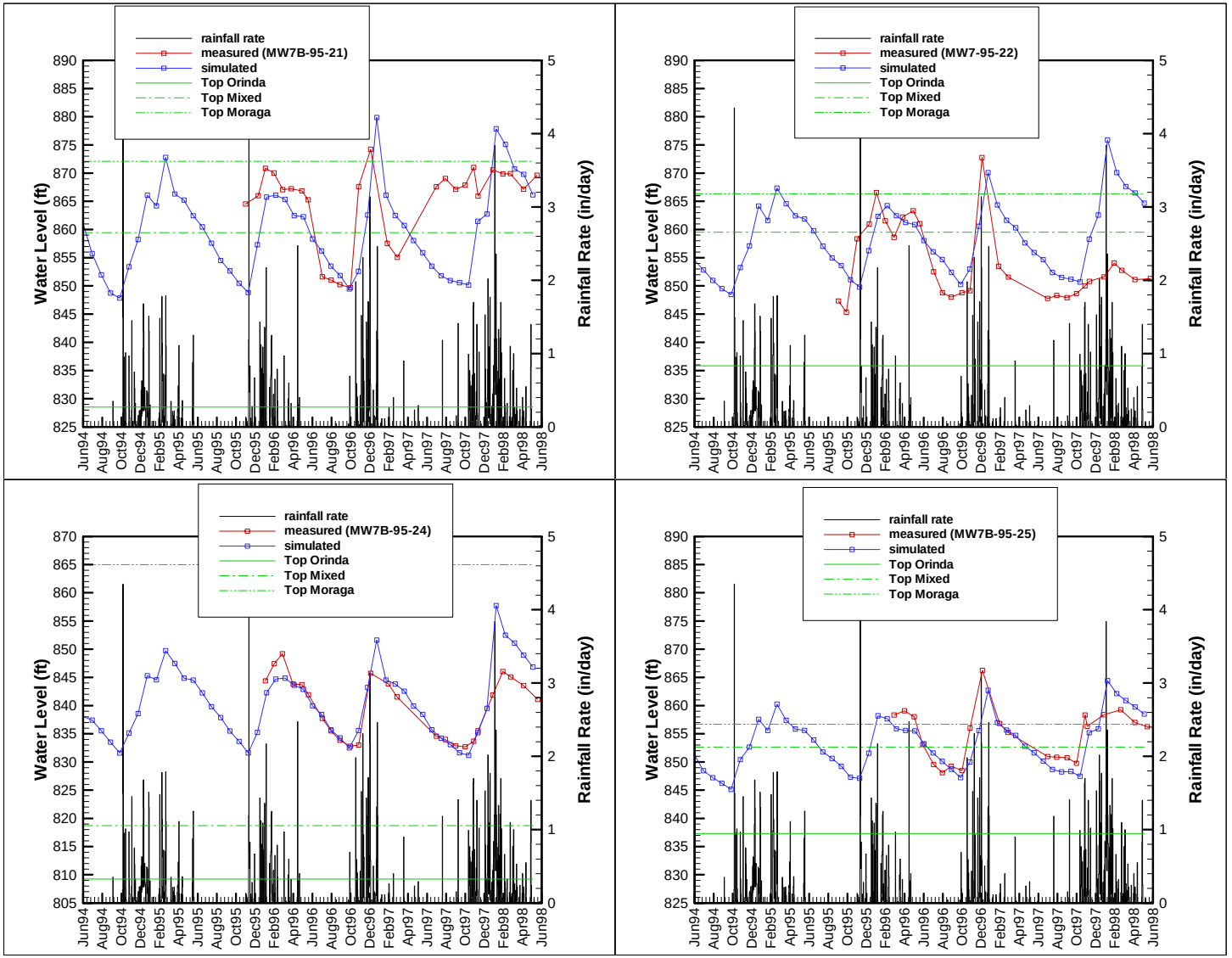

Figure 32. Match between the simulated and measured water levels at four monitoring wells in the Building 7 subsystem.

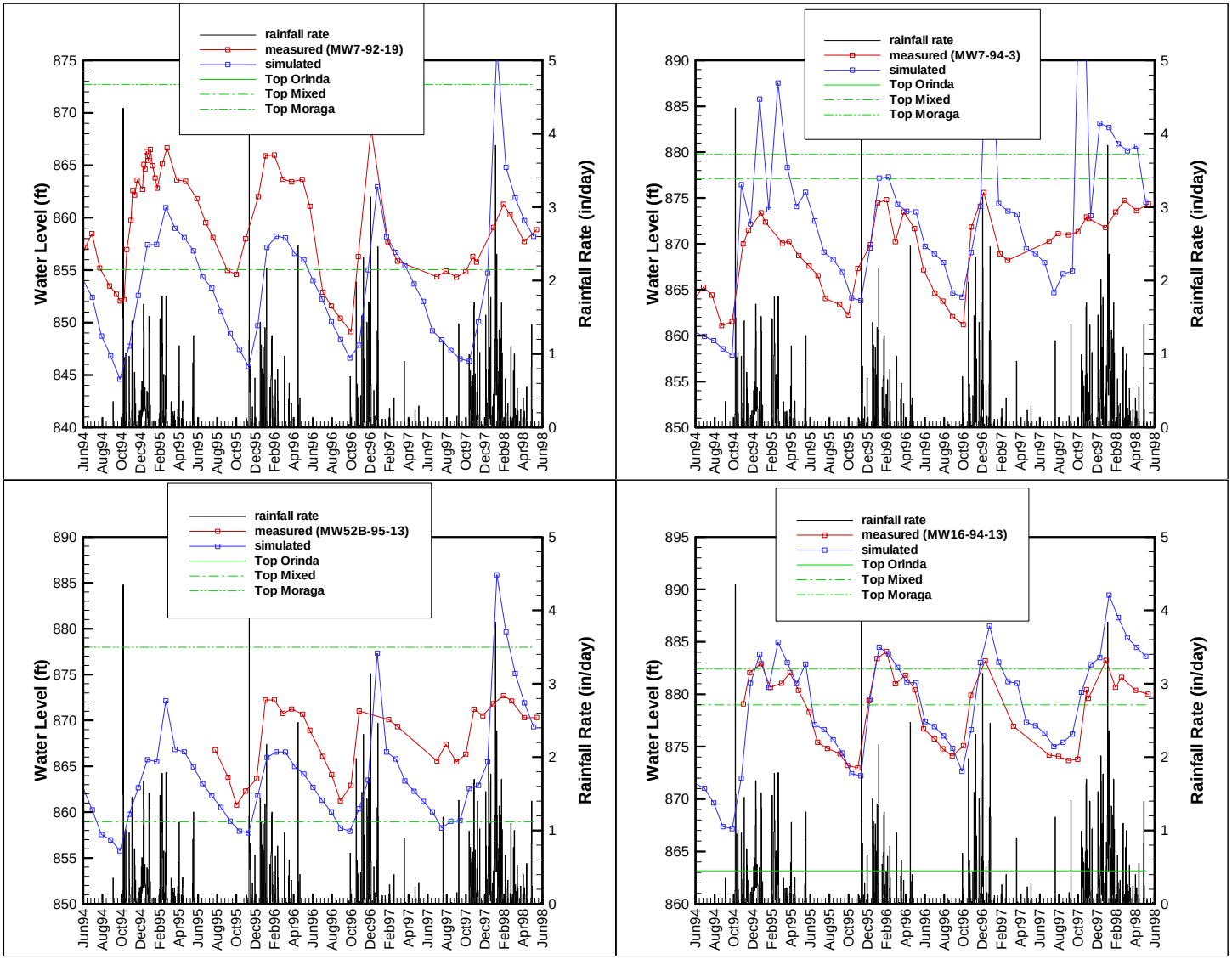

Figure 33. Match between simulated and measured water levels at four monitoring wells in the Building 7 subsystem (cont.).

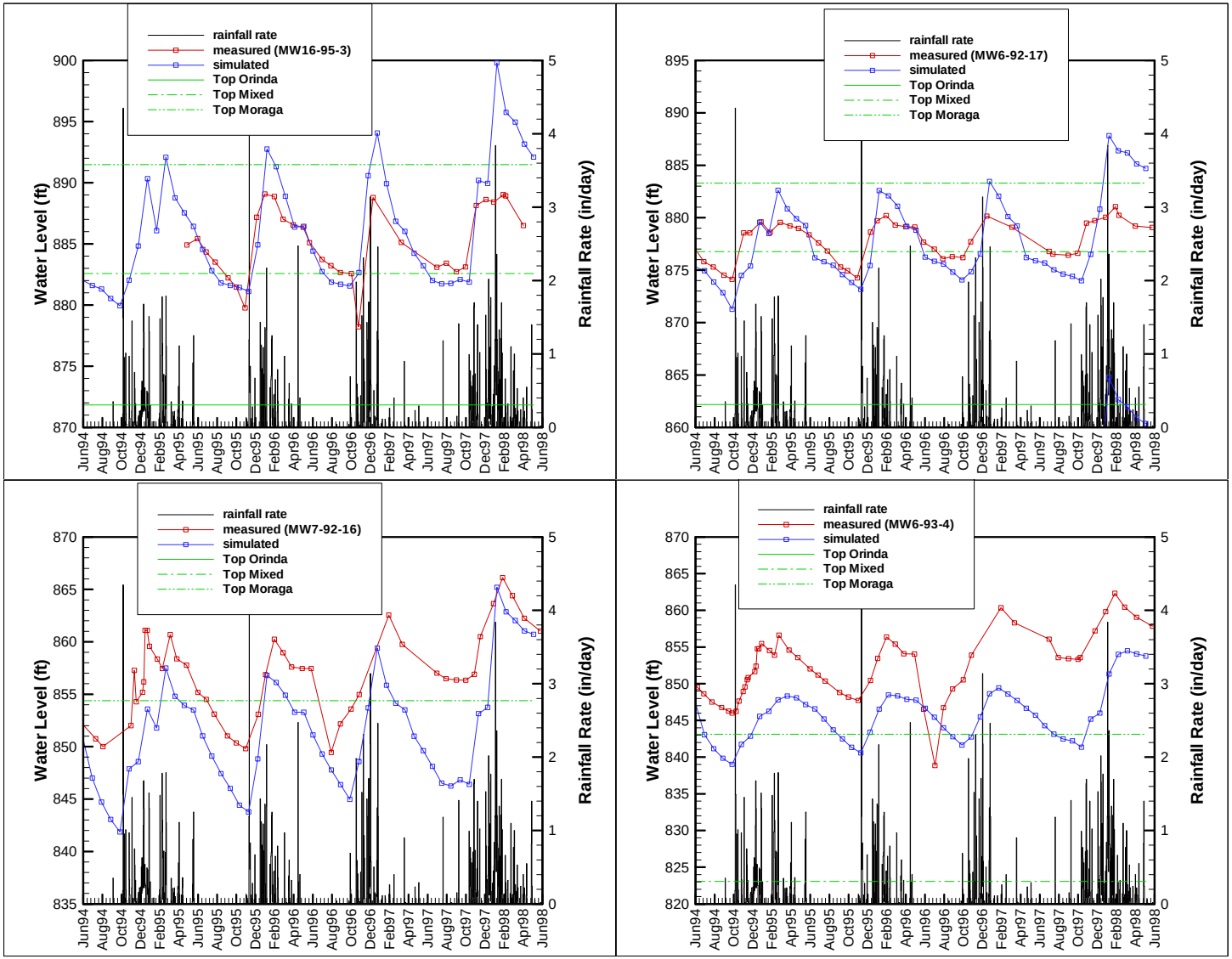

Figure 34. Match between the simulated and measured water levels at four monitoring wells in the Small-Moraga-Bowl subsystem.

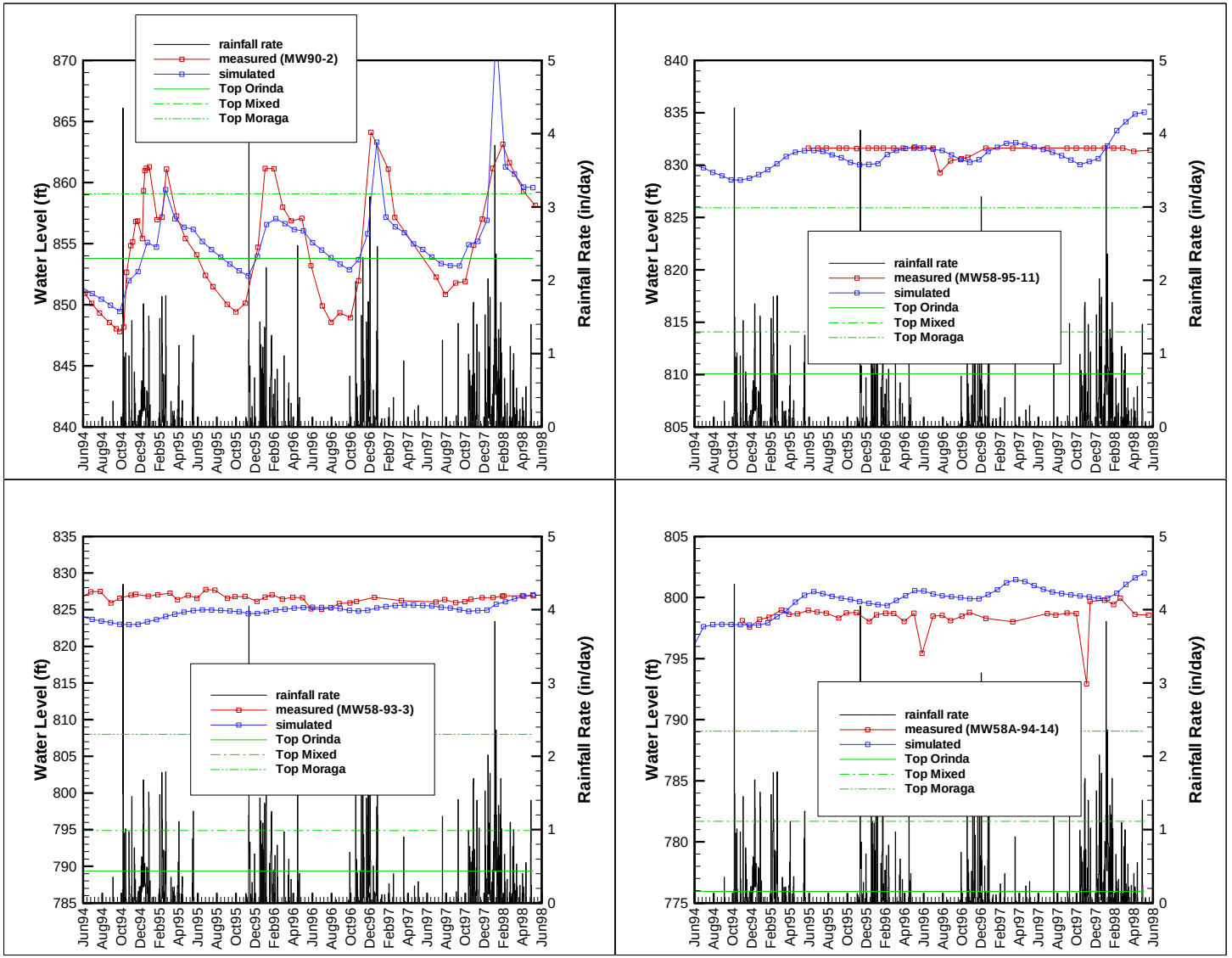

Figure 35. Match between the simulated and measured water levels at four monitoring wells in the Small-Moraga-Bowl subsystem (cont.).

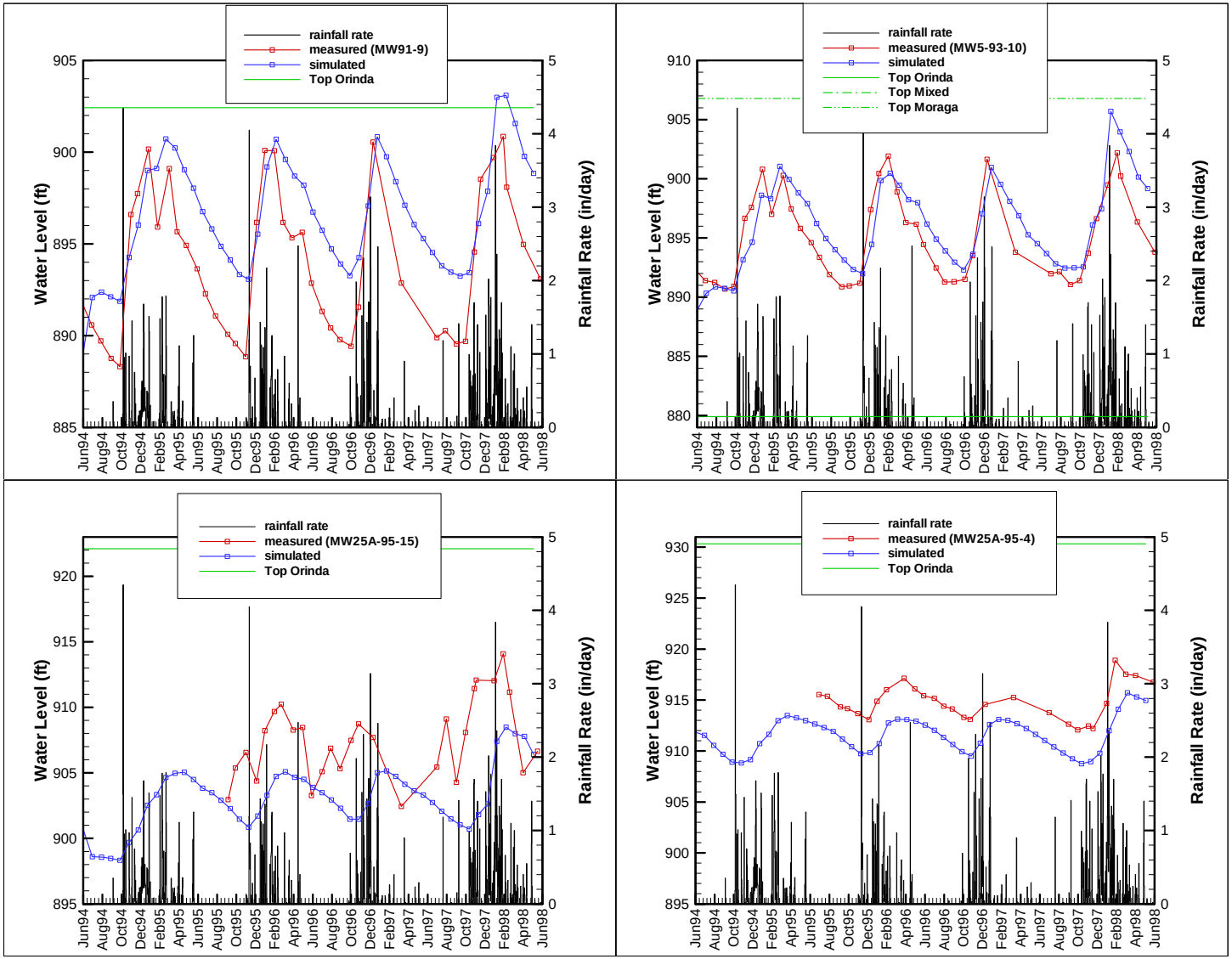

Figure 36. Match between the simulated and measured water levels at four monitoring wells in the South-Orinda subsystem.

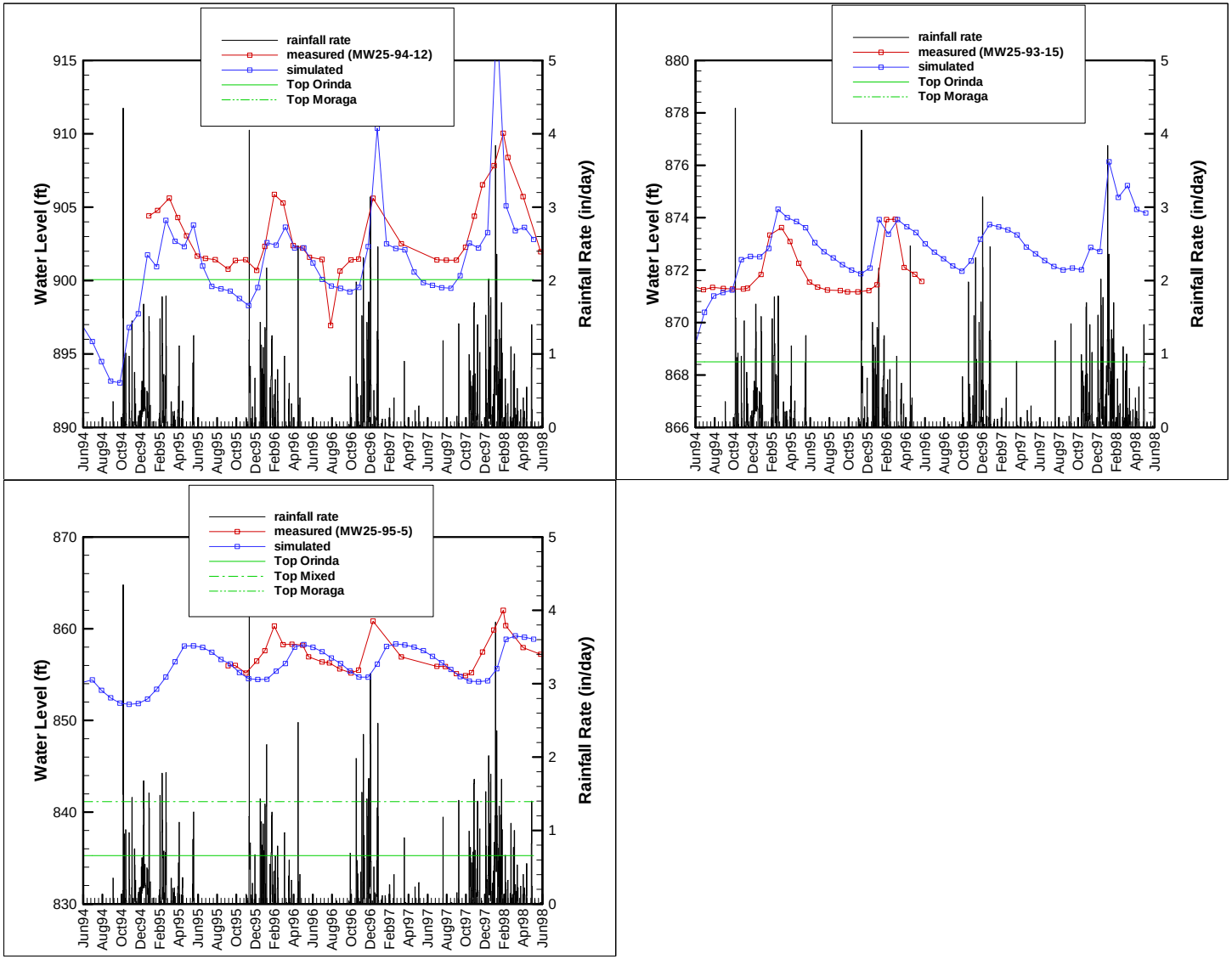

Figure 37. Match between the simulated and measured water levels at four monitoring wells in the South-Orinda subsystem (cont.).

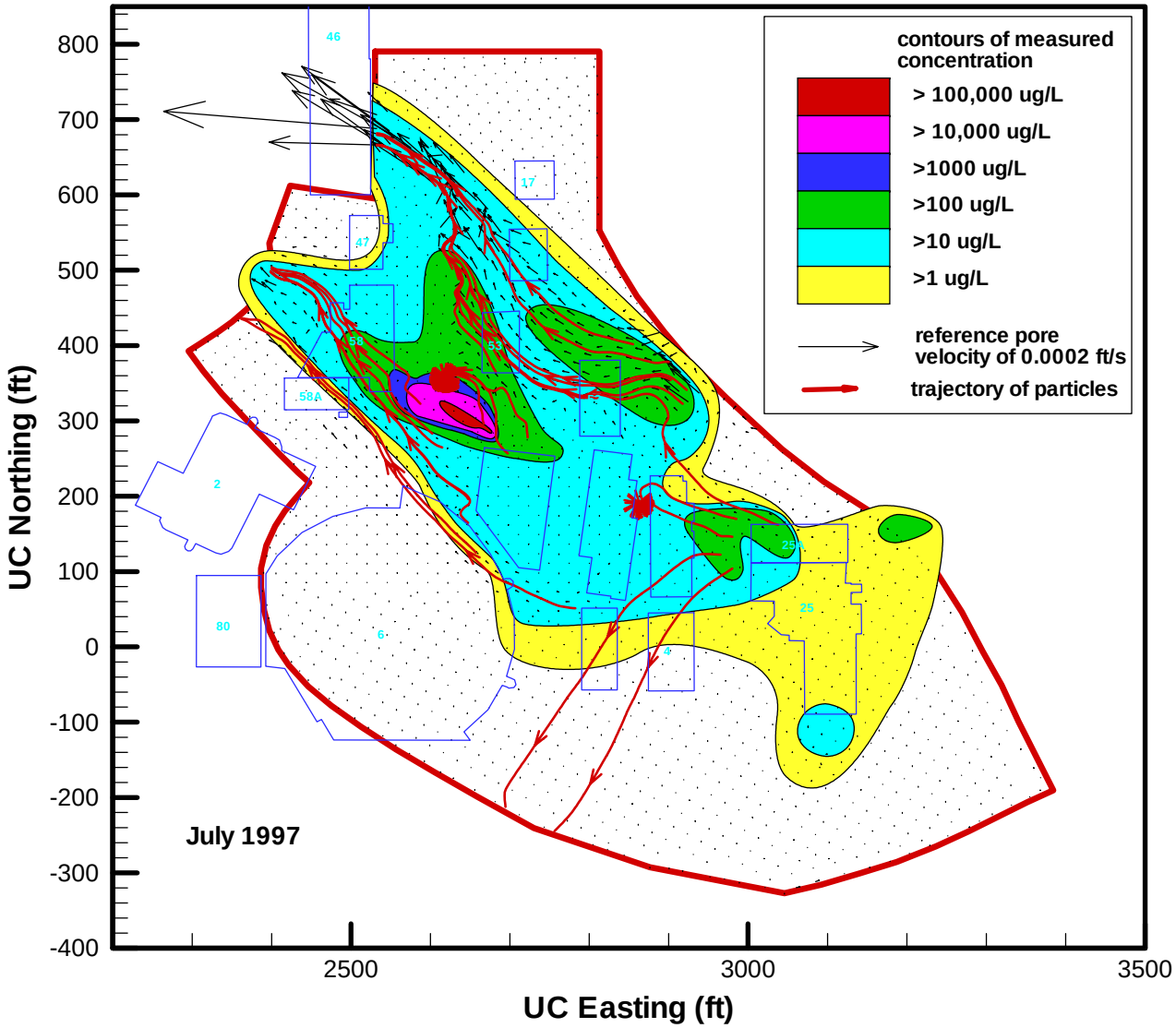

Figure 38. Trajectories of particles originating from the contaminant source areas at B7 lobe, B52 lobe, and B25A lobe. These trajectories are obtained using the steady-state flow in the dry season with pore velocity at July 1997.

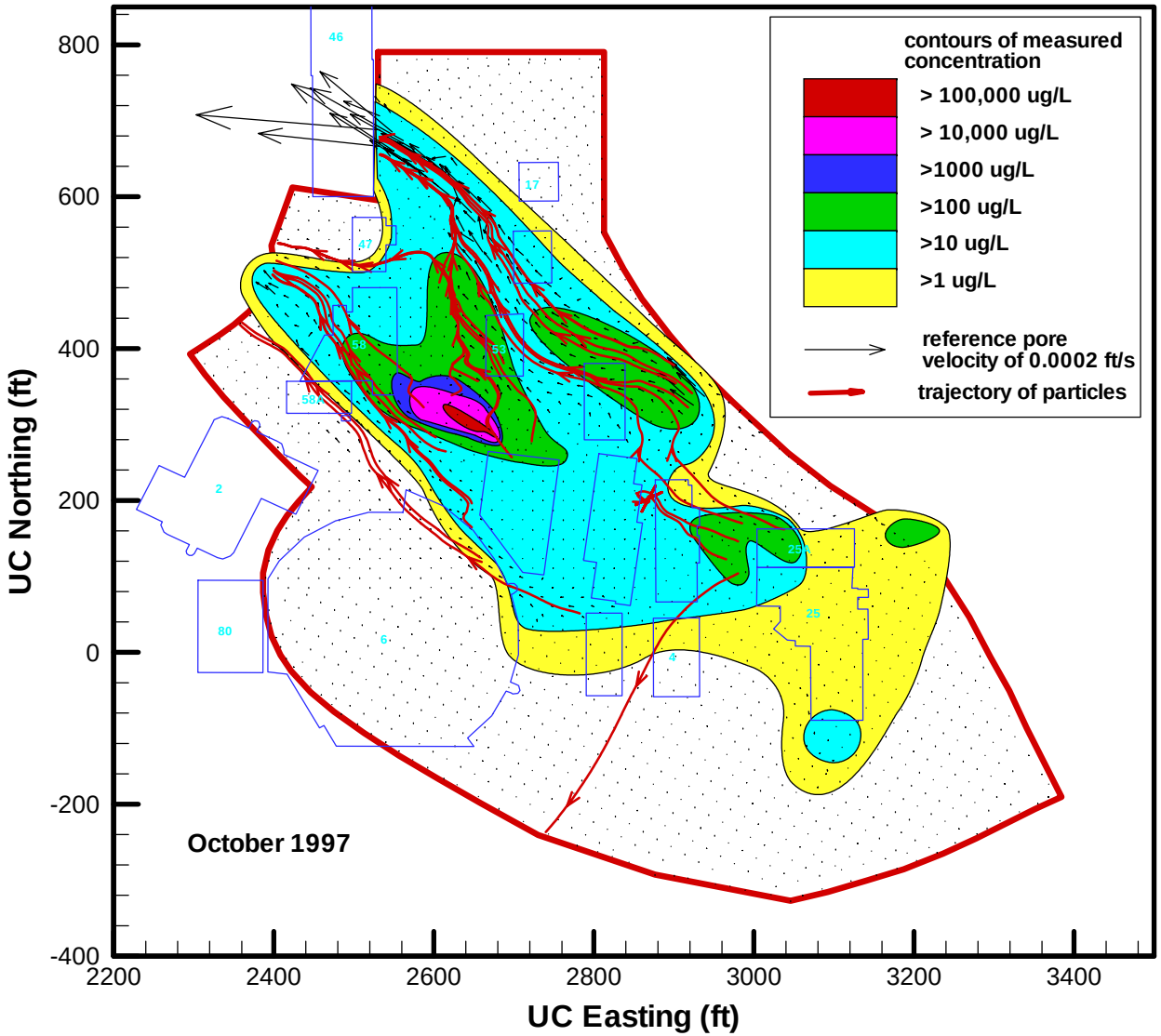

Figure 39. Trajectories of particles originating from the contaminant source areas at B7 lobe, B52 lobe, and B25A lobe. These trajectories are obtained using the steady-state flow in the wet season with pore velocity at October 1997.

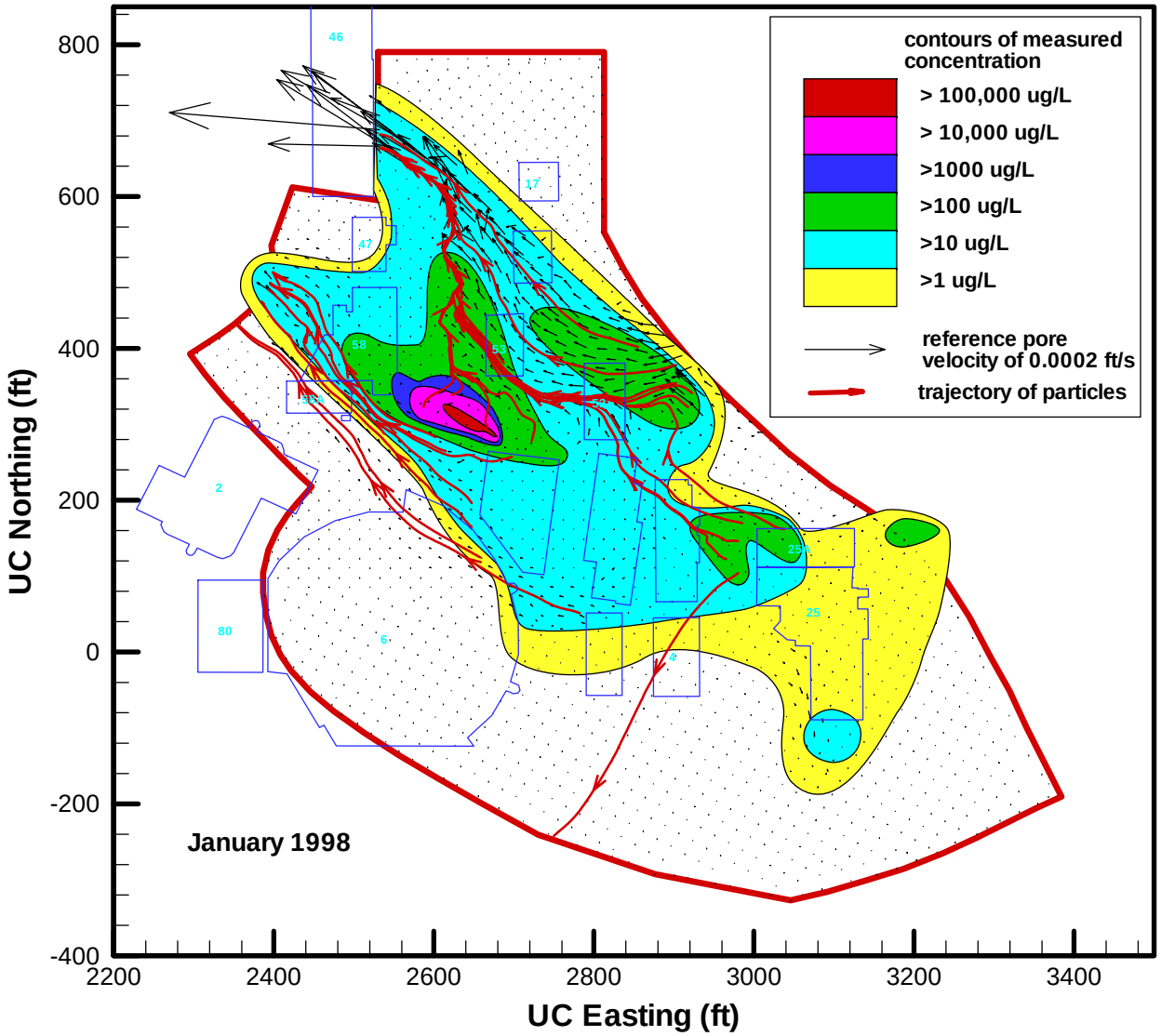

Figure 40. Trajectories of particles originating from the contaminant source areas at B7 lobe, B52 lobe, and B25A lobe. These trajectories are obtained using the steady-state flow in the wet season with pore velocity at January 1998.

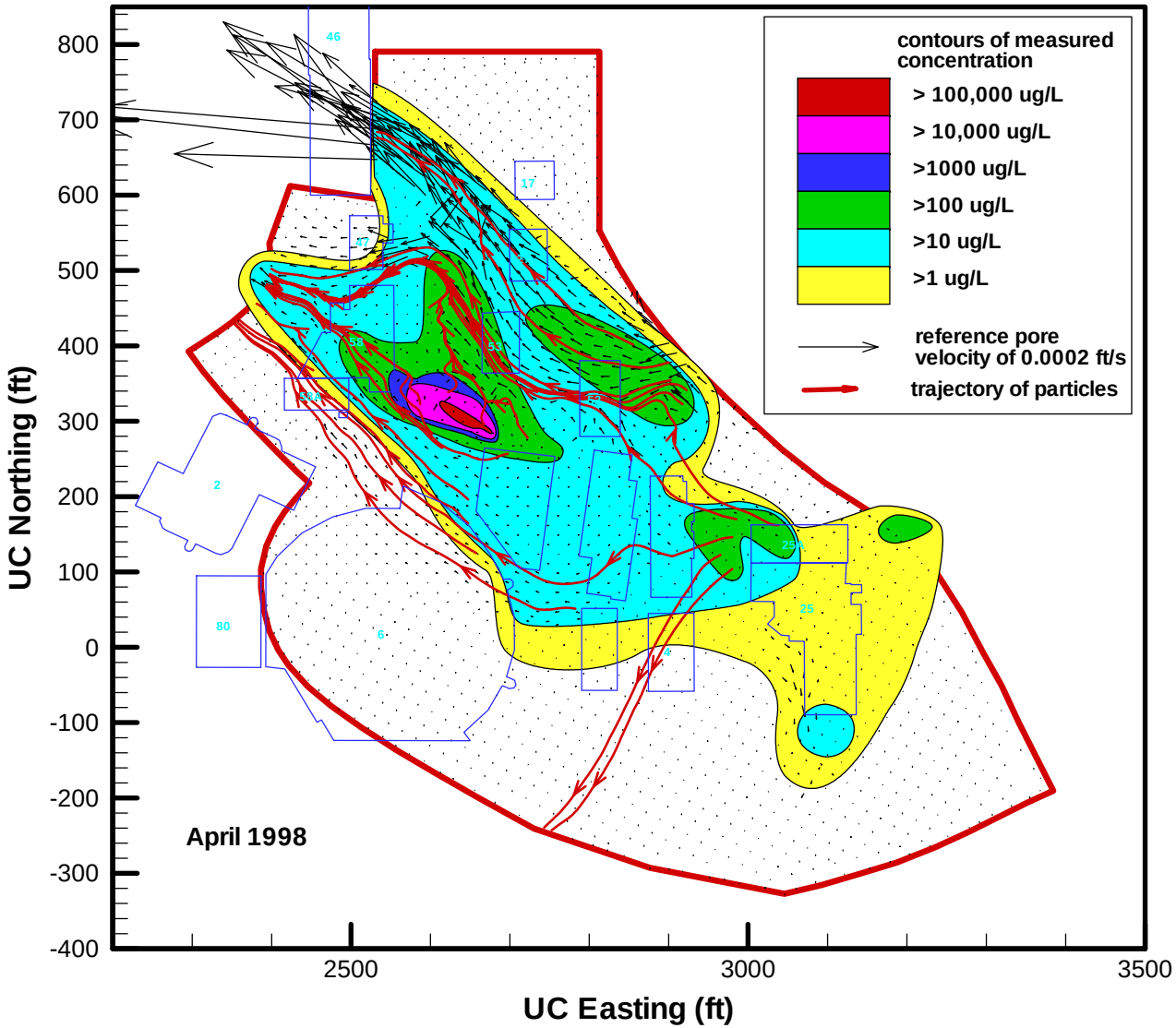

Figure 41. Trajectories of particles originating from the contaminant source areas at B7 lobe, B52 lobe, and B25A lobe. These trajectories are obtained using the steady-state flow in the wet season with pore velocity at April 1998.

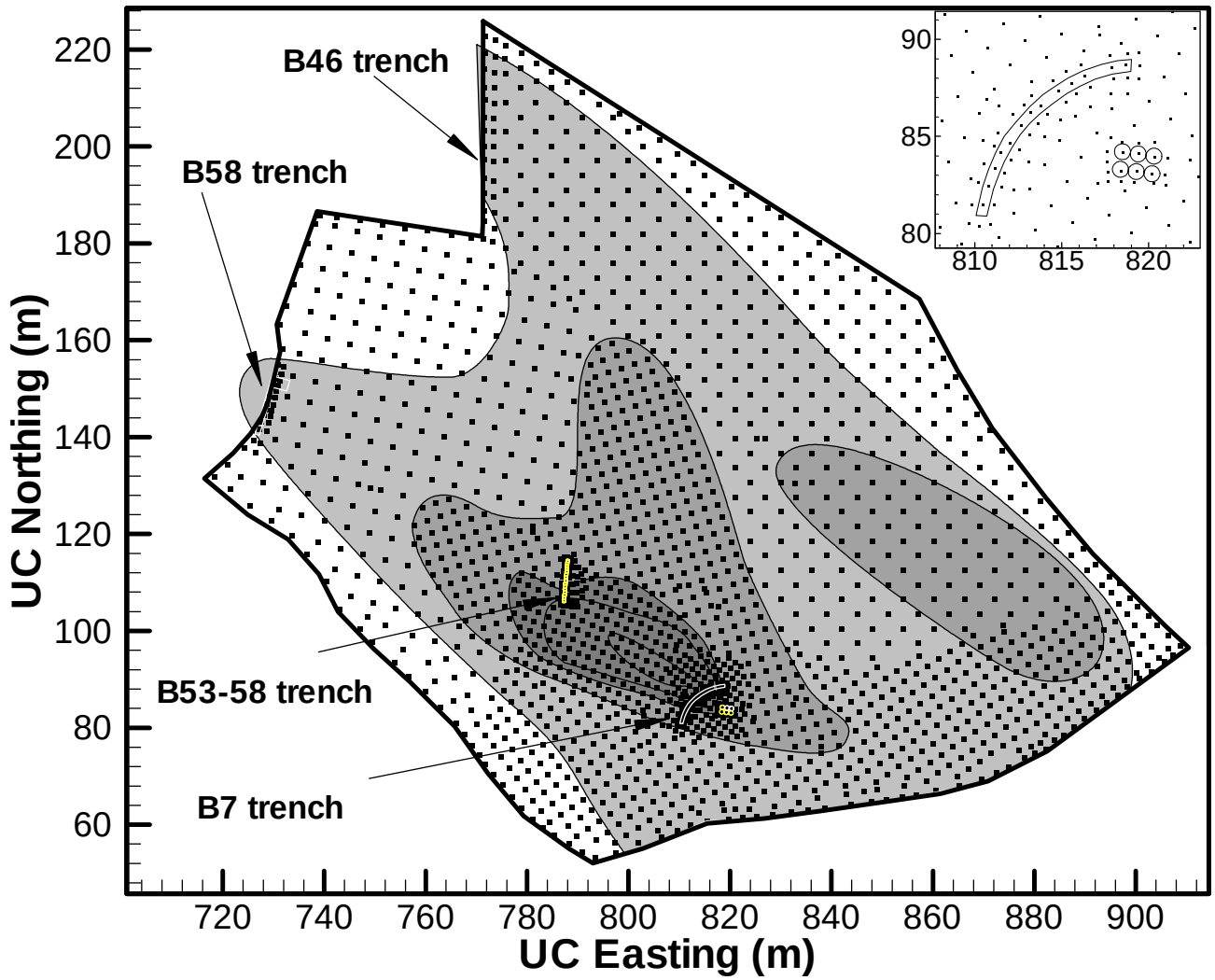

Figure 42. Boundary and plan view of the three-dimensional mesh for the refined model, showing the four trenches implemented for restoration. The background is the measured concentration contour with the contour legend shown in Figure 41. The right upper-corner plot shows a close-up view of the sump and the B7 trench system for controlling the contaminant source.

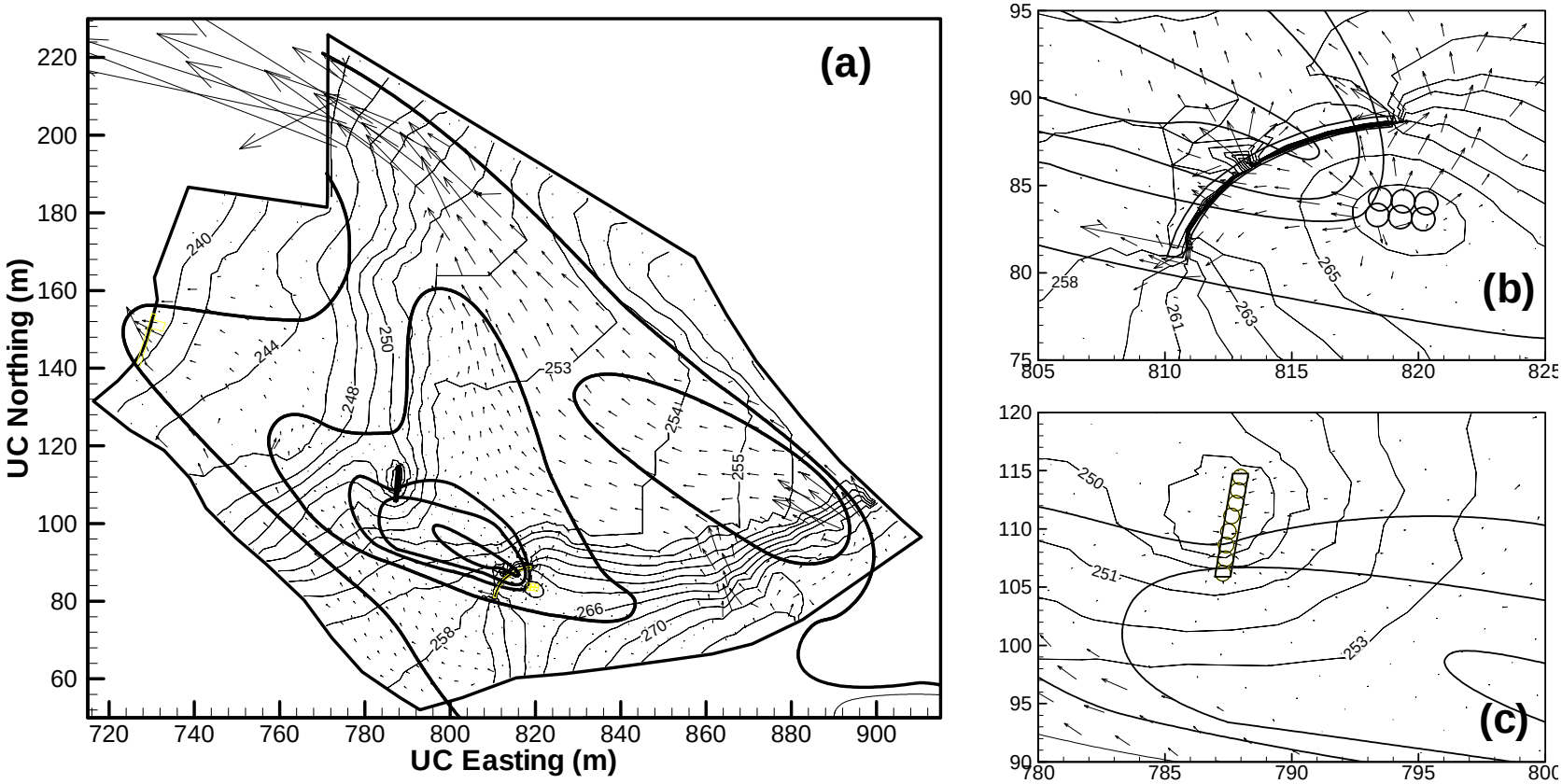

Figure 43. Contour of the predicted groundwater level (light lines) and flow velocity vector fields on the water table in October 1999 for the refined model in (a) the entire model domain, (b) in the vicinity of the B7 trench, and (c) in the vicinity of the B53-B58 trench. Note that the contaminant plume contour lines are indicated by thick lines (for scales, see Figure 41).